Inverse modelling of the spatial distribution of NOx emissions on a continental scale using satellite data

I. B. Konovalov, Matthias Beekmann, A. Richter, J. P. Burrows

Atmos. Chem. Phys., 6, 1747–1770, 2006
www.atmos-chem-phys.net/6/1747/2006/

Atmospheric Chemistry and Physics

Inverse modelling of the spatial distribution of NO_x emissions on a continental scale using satellite data

I. B. Konovalov[1,2], **M. Beekmann**[2], **A. Richter**[3], **and J. P. Burrows**[3]

[1]Institute of Applied Physics, Russian Academy of Sciences, Nizhniy Novgorod, Russia
[2]Laboratoire Inter-Universitaire de Systèmes Atmosphériques, CNRS, Créteil, France
[3]Institute of Environmental Physics and Remote Sensing, IUP/IFE, University of Bremen, Bremen, Germany

Received: 7 September 2005 – Published in Atmos. Chem. Phys. Discuss.: 8 December 2005
Revised: 9 March 2006 – Accepted: 27 March 2006 – Published: 24 May 2006

Abstract. The recent important developments in satellite measurements of the composition of the lower atmosphere open the challenging perspective to use such measurements as independent information on sources and sinks of atmospheric pollutants. This study explores the possibility to improve estimates of gridded NO_x emissions used in a continental scale chemistry transport model (CTM), CHIMERE, by employing measurements performed by the GOME and SCIAMACHY instruments. We set-up an original inverse modelling scheme that not only enables a computationally efficient optimisation of the spatial distribution of seasonally averaged NO_x emissions (during summertime), but also allows estimating uncertainties in input data and a priori emissions. The key features of our method are (i) replacement of the CTM by a set of empirical models describing the relationships between tropospheric NO_2 columns and NO_x emissions with sufficient accuracy, (ii) combination of satellite data for tropospheric NO_2 columns with ground based measurements of near surface NO_2 concentrations, and (iii) evaluation of uncertainties in a posteriori emissions by means of a special Bayesian Monte-Carlo experiment which is based on random sampling of errors of both NO_2 columns and emission rates. We have estimated the uncertainty in a priori emissions based on the EMEP emission inventory to be about 1.9 (in terms of geometric standard deviation) and found the uncertainty in a posteriori emissions obtained from our inverse modelling scheme to be significantly lower (about 1.4). It is found also that a priori NO_x emission estimates are probable to be persistently biased in many regions of Western Europe, and that the use of a posteriori emissions in the CTM improves the agreement between the modelled and measured data.

Correspondence to: I. B. Konovalov
(konov@appl.sci-nnov.ru)

1 Introduction

As a result of recent impressive developments in the satellite measurements of the atmosphere (see, e.g. Burrows, 1999; Bovensmann et al., 1999; Levelt, 2000), this type of measurements provides now plentiful and novel information also on the composition of the lower atmosphere. In particular, tropospheric column amounts of several important trace gases such as NO_2, CH_4, SO_2, BrO, HCHO (e.g., Velders et al., 2001; Richter and Burrows, 2002; Buchwitz et al., 2004; Eisinger and Burrows, 1998; Wagner and Platt, 1998) have been derived from these observations. In view of these developments, one of the challenging opportunities is to use satellite data for the estimation of sources of atmospheric gases by means of inverse modelling. It seems reasonable to expect that the almost global satellite measurements performed with fairly high spatial and temporal resolution bear much more information on sources of trace gases than the observational data that could be provided by relatively sparse ground based networks.

This study examines the possibility to use satellite data for tropospheric NO_2 columns in order to improve existing estimates for the spatial distribution of emissions of nitrogen oxides (NO_x). The tropospheric NO_2 columns derived from satellite measurements have already been used for the estimation of NO_x emissions on the global scale (Leue et al., 2001; Martin et al., 2003; Müller and Stavrakou, 2005; Toenges-Schuller, 2005). However, since satellite measurements are available in much higher spatial resolution than the typical resolution of global models, the information provided by satellite observations cannot be fully exploited by global models. Moreover, finer spatial scales than those typically considered in the global models are addressed in air quality studies. Accordingly, there is a challenging perspective to use satellite measurements in order to improve emission data which are employed in air quality models. In this study, we

Published by Copernicus GmbH on behalf of the European Geosciences Union.

use the satellite data from the GOME and SCIAMACHY instruments together with a continental scale chemistry transport model (CTM) CHIMERE that has been originally designed for simulations of photo-oxidant pollution.

Oxides of nitrogen, being very reactive gases, play an important role in the chemistry of both the boundary layer and free troposphere (e.g., Kley et al., 1999; Bradshaw et al., 2000) and contribute to radiative forcing of the climate (Solomon et al., 1999; Velders et al., 2001). Accordingly, the knowledge of NO_x sources is required both for an adequate description of the present and future state of the atmospheric composition. Inverse modelling offers a way to validate and improve the existing emission estimates provided by traditional emission inventories.

Inverse modelling of sources of atmospheric gases is a well-established area of atmospheric research, which is now treated in numerous publications (see, e.g., Enting, 2002, for an overview). The main idea of the inverse modelling is that improved source estimates can be derived by optimisation of emission parameters using available observations as constraints to the model output. However, the practical implementations of this idea meet some general problems (Enting, 2002). One of the major problems concerns the estimation and treatment of uncertainties in input data and output results. While this kind of problems is rather common for natural science in general, it is especially important in inverse modelling studies, because the uncertainties in the observational data and errors of a model tend to be amplified in the derived emission estimates. The reason for this amplification is that, due to the discrete character of measurements and due to irreversible mixing in the atmosphere, the information provided by real observations of trace gases, is usually insufficient for unambiguous retrieval of their sources.

The common way to handle this problem is to use a probabilistic approach, which enables minimization of uncertainties in obtained estimates via the optimal combination of observational and a priori information (Tarantola, 1987). In order to implement this approach, one has to quantify uncertainties in input data (observations and a priori estimates of emissions) and also the part of model uncertainties which is not caused by emission uncertainties. It is recognised that these uncertainties are crucial parameters of inverse modelling schemes (Kaminski, 1999; Heimann and Kaminski, 1999). However, even if the uncertainties in observations may, to some degree, be known (for example, when they are performed by in situ methods), generally only crude estimates for uncertainties in the model and in a priori emission data can be made. If uncertainties are evaluated inaccurately, the weight (confidence) attributed either to observations or to a priori information may be wrong and results may be biased.

Another major problem of inverse modelling studies is their large computational demand. Optimisation of parameters is much more costly as simple forward runs, even if it is performed using special methods such as adjoint models (Giering, 2000). The computational demand becomes even much larger when non-linearity between observational data and emissions is allowed, since then evaluating uncertainties necessitates multiple reiterations of the optimisation procedure (Müller and Stavrakou, 2005).

While the majority of inverse modelling studies performed so far dealt with chemically inert (CO_2) or slowly reacting (CO, CH_4) species (e.g., Kaminski, 1999; Petron et al., 2002; Houweling et al., 1999) inverse modelling of such reactive species as nitrogen oxides is a rather new area of research. The most relevant earlier studies have already been mentioned above. Specifically, Leue et al. (2001) have pioneered the inverse modelling of NO_x emissions on the global scale using data from satellite (GOME) measurements. They derived the estimates of NO_x emissions for several large regions of the world by assuming a constant NO_x lifetime of 27 h. Martin et al. (2003) have performed more accurate inverse modelling of NO_x emissions on the global scale using GOME data together with a global CTM. They used NO_x lifetime estimated independently for each model grid cell under the assumption that the transport of NO_2 between neighbouring grid cells could be neglected. They also reduced the uncertainties of their "top-to-down" emissions estimates by combining them with the data of "bottom-to-up" NO_x emission inventories. More recently, Müller and Stavrakou (2005) have performed the coupled inversion of CO and NO_x emissions aggregated for several regions of the world using GOME NO_2 data together with data of CO ground based measurements. Finally, Toenges-Schuller (2005) has performed a systematic statistical analysis and comparison of different data sources relative to the global distribution of NO_x emissions (EDGAR data, night-time lights as a proxy for NO_x emissions and NO_x emission estimates derived from GOME measurements assuming the direct relationships between NO_x emissions and NO_2 columns in each grid cell). The important novel feature of her study is an attempt to estimate uncertainties in different emission data by considering their covariations.

In our study we perform inverse modelling of NO_x emissions for Western Europe, taking advantage of the higher spatial resolution typical for a continental scale CTM (1/2 deg.). The main objective of our study is to explore the possibility to improve the current knowledge of the spatial structure of NO_x emissions by using satellite data. The key questions that should be answered in order to reach a valid conclusion concern the uncertainties in satellite data, in model outputs, and in available "bottom-up" emissions inventories. For example, if the available emission estimates were sufficiently accurate but the satellite data were very uncertain, then the satellite measurements would be essentially useless for improving emissions. Unfortunately, all uncertainties mentioned above are essentially unknown. In particular, the satellite data for tropospheric NO_2 columns are obtained as a result of rather complex procedure that involves not only measured characteristics but also a number of assumptions and model results. Even if the level of uncertainty of a single

retrieval can, in principal, be roughly estimated by means of the error propagation analysis (Boersma et al., 2004), it still remains unknown to which degree these uncertainties can be reduced when one considers NO_2 columns averaged over a period of several months. Similarly, although the uncertainties of NO_x emission inventories have been evaluated for certain types of sources and certain countries (e.g., Kühlwein and Friedrich, 2000; Kühlwein et al., 2002), practically no reliable information is yet available on uncertainties in the gridded emissions used in continental scale CTMs.

One of the main ideas in this study is to set up a special procedure to obtain independent estimates for the above mentioned uncertainties. To this purpose, additional observational data is considered in parallel to satellite observations, i.e. near surface NO_2 concentrations gathered within the EMEP network. As a result, our inverse modelling procedure involves only a minimum of unavoidable assumptions concerning general statistical error properties.

Another important feature of our study is the original method that is employed in order to reduce the computational demand of the considered problem. It is shown that it is possible to replace the original CTM by a set of simple statistical models that describe a linear relationship between relative perturbations of NO_2 columns and NO_x emissions. Note that, in contrast to Martin et al. (2003) and Toenges-Schuller (2005), we take into account to a certain extent NO_2 transport between different model grid cells because it plays a significant role on the scales considered in our study.

The paper is organised as follows. A brief description of the CHIMERE CTM and an overview over observational and modelled data are given in Sect. 2. Section 3 describes our inversion scheme and presents some tests with synthetic data. Results obtained with real data are presented and discussed in Sect. 4. The concluding section summaries our main findings.

2 Model and data description

2.1 Chemistry transport model CHIMERE

CHIMERE is a Eulerian multi-scale CTM designed for studying various air pollution related issues. An in-detail model description, a technical documentation and source codes are available on the web (http://euler.lmd.polytechnique.fr/chimere/) and can also be found in literature (see, e.g., Schmidt et al., 2001; Vautard et al., 2001, 2003; Beekmann and Derognat, 2003; Bessagnet et al., 2004). Accordingly, only the major model features and those specific for the present study are outlined below.

The CHIMERE domain used in this study covers most of Western Europe (from 10° W to 20° E and from 40° N to 55° N) with a horizontal resolution of $0.5\times0.5°$ and includes 1800 grid cells. In the vertical, the model has 8 layers defined by hybrid coordinates. The top of the upper layer is fixed at the 500 hPa pressure level.

Meteorological input data are calculated off-line using the non-hydrostatic meso-scale model MM5 (http://www.mmm.ucar.edu/mm5/) that is run on a regular grid with horizontal resolution of 100×100 km. MM5 is initialized and driven with NCEP Re-Analysis-2 data (http://www.cpc.ncep.noaa.gov/products/wesley/ncep_data/).

The chemical scheme used in this study (Schmidt et al., 2001; Derognat, 2002) was derived from the more complete MELCHIOR chemical mechanism (Latuatti, 1997) using the concept of chemical operators (Carter, 1990; Aumont et al., 1997). It includes 44 species and about 120 reactions. Lateral boundary conditions are specified using monthly average values of a climatological simulation of the second generation MOZART model (Horowitz et al., 2003).

Photolysis rates are calculated using the tabulated outputs from the Troposphere Ultraviolet and Visible model (TUV, Madronich and Flocke, 1998) and depend on altitude and zenith angle. Radiation attenuation due to clouds is taken into account under the assumption that the processes considered in the model take place below the top of the cloud layer. Accordingly, the clear sky photolysis rates are scaled with a radiation attenuation coefficient that is calculated as a function of cloud optical depth.

The anthropogenic emissions for NO_x, SO_2, CO, and non-methane volatile organic compounds (NMVOC) are specified using the 2001 EMEP yearly data distributed to 11 Selected Nomenclature for Air Pollution (SNAP) sectors (see EMEP-CORINAIR Emission Inventory Guidebook (2005) for sector definitions) and gridded with horizontal resolution of 50×50 km. The data provided by IER, University of Stuttgart (GENEMIS, 1994) are used to define daily, weekly, and seasonal variations of emissions. Note that the model does not take into account emissions from aircrafts. Such emissions are believed to provide rather insignificant fraction (1–2%) of total anthropogenic emissions both on the global and European scales (e.g., Lee et al., 2005; Tarassón et al., 2004).

The evaluation of biogenic emissions of isoprene, terpenes and NO is based on methodologies and data presented in respectively Simpson et al. (1999) and Stohl et al. (1996). The NO_x emissions from lightning are not included. While lightning is believed to provide important contribution of NO_x in tropical regions (e.g., Labrador et al., 2005), this source of NO_x is on the average much smaller for Europe. Specifically, in accordance to estimates by Boersma et al. (2005), the lightning produced average NO2 column amount over Europe in summer season is likely less than 8×10^{13} (molecules/cm^2), while the total NO_2 column amount over Europe (this study) is, on the average, 2.9×10^{15} (molecules/cm^2). Emission rates from anthropogenic and biogenic sources calculated in CHIMERE are shown in Fig. 1. In accordance to these calculations, anthropogenic emissions tend to be dominating over most parts of

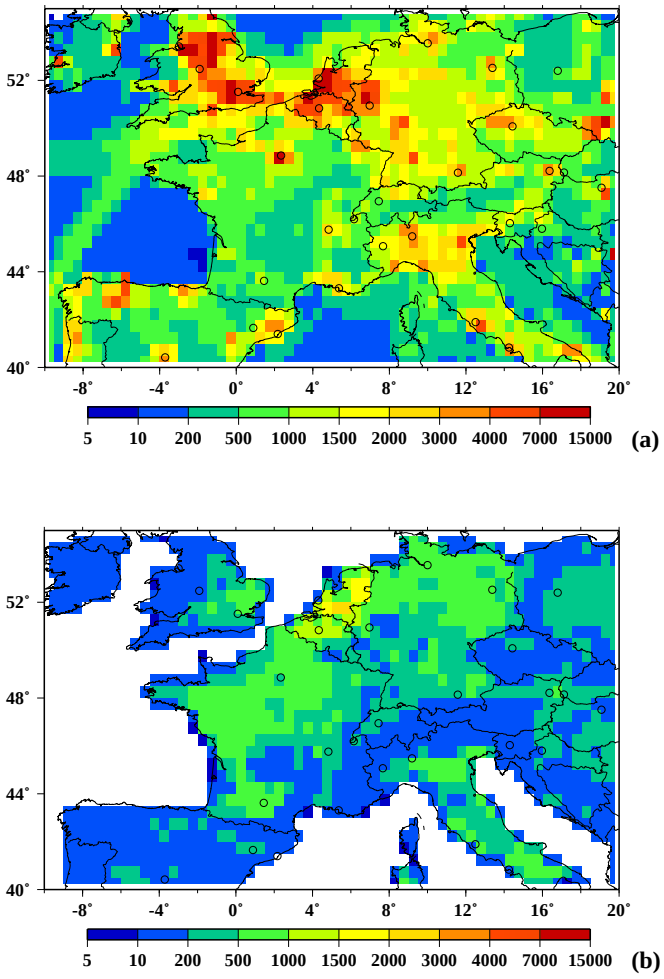

Fig. 1. The anthropogenic **(a)** and biogenic **(b)** emission rates (in molecules$\times$cm$^{-2}\times$s$^{-1}\times10^8$) specified in CHIMERE. The data shown are averages over three summer months (June–August) of 2001.

Western Europe, although there are some regions (for example, in France), where the anthropogenic and biogenic emissions (during the warm season) are of the same order of magnitude.

In this study, CHIMERE is used to simulate tropospheric NO_2 column amounts and near surface concentrations for the summer months (June–August) of 2001. The choice of summer months has been motivated by the fact that CHIMERE is designed, primarily, for simulating photo-oxidant pollution during the warm season. Besides, the shorter lifetime of NO_x during the warm season facilitates a technical solution of the inverse modelling problem. In order to be consistent with satellite data, which will be described in the next section, the modelled NO_2 columns for each model grid cell are taken between 10 and 11 h of local solar time and only on days with insignificant cloud cover. Since the total cloud cover is not used in the CHIMERE simulation, we use a selection criteria based on a threshold value of the radiation attenuation coefficient. Specifically, we disregarded days on which reduction of solar radiation due to clouds was larger than 30%. Although this selection criterion does not insure the exact agreement between the selected days and the days on which the data of satellite observations were actually available, a possible inconsistency is expected to be small, particularly because we perform averaging of the selected data for three summer months (June-August). Such averaging enables compensating of random inconsistencies between GOME and CHIMERE on different days. This expectation is confirmed by results of special tests in which the sensitivity of simulated seasonally average NO_2 columns to the day selection criterion has been found to be insignificant.

The potential uncertainties in simulated tropospheric NO_2 columns due to omission of the upper troposphere have been considered in Konovalov et al. (2005). In particular, it has been shown that the spatial variability of tropospheric NO_2 above 500 hPa pressure level contributes only very insignificantly to the spatial variability of total tropospheric NO_2 columns. The respective systematic bias in simulated NO_2 columns is more significant (about 19 percent on the average). However, as it is argued below, the results of this study are not sensitive to systematic uncertainties in the measured and simulated data.

2.2 Satellite data

We used the data for tropospheric NO_2 columns derived from measurements performed by Global Ozone Monitoring Experiment (GOME) spectrometer on board of the second European Research Satellite (ERS-2) and the Scanning Imaging Absorption spectroMeter for Atmospheric ChartographY (SCIAMACHY) on board of the Envisat satellite. These data are scientific products of the University of Bremen.

The GOME instrument is a grating pseudo double monochromator covering the wavelength range from 280 to 790 nm with the spectral resolution of 0.2–0.4 nm (Burrows et al., 1999). NO_2 concentrations are retrieved from irradiances in a spectral window from 425 to 450 nm. The typical ground pixel size is 320 km across the track of the satellite (i.e., in West-East direction), and 40 km along the track. The orbit of ERS-2 is sun-synchronous near-polar orbit with an equator crossing time of 10:30 LT in the descending node. The nearly total coverage of measurements is reached in three days.

SCIAMACHY is a passive remote sensor designed to detect electromagnetic radiation in the spectral range from 240 and 2380 nm with a spectral resolution between 0.2 and 1.5 nm (Bovensmann et al., 1999). The NO_2 columns have been retrieved using measurements in the spectral window from 425 to 450 nm where the resolution of the instrument is about 0.4 nm. SCIAMACHY operates in both nadir and limb modes. Only measurements performed in the nadir mode

have been used to retrieve NO_2 columns for this study. The typical horizontal resolution of the instrument in the nadir mode is about $30\times60\,km^2$. ENVISAT flies in a sun synchronous near polar orbit with the equator crossing time in the descending node at 10:00 a.m. of local time. Global coverage is achieved after 6 days.

The methods of retrieval of tropospheric NO_2 columns from the irradiance spectrum measured by satellite instruments have been discussed in numerous papers (see, e.g., Richter and Burrows, 2002; Martin et al., 2002; Boersma et al., 2004; Heue et al., 2005). The algorithms used in different studies follow the same principles, although they may differ in details. Specifically, tropospheric NO_2 columns are obtained in several steps, including the retrieval of slant column amounts by means of DOAS (Differential Optical Absorption Spectroscopy) method (Richter, 1997), the estimation of the stratospheric part of the slant columns and the evaluation of tropospheric air mass factors (AMF) that describe the light path in the troposphere and are used to convert the tropospheric slant columns to vertical columns. The evaluation of AMF involves estimations of the vertical distribution of NO_2 in the troposphere and the surface albedo as well as assumptions regarding scattering and absorption of the light on aerosols and clouds.

The GOME NO_2 columns utilized in this study have been retrieved with the same method as those used in our earlier study (Konovalov et al., 2005), in which the tropospheric NO_2 columns derived from GOME measurements were analysed together with NO_2 columns simulated by CHIMERE. The distinctive features of this method are (1) the estimation of a stratospheric part of the slant columns based on simulations with the global CTM SLIMCAT (Chipperfield et al., 1999), (2) the use of NO_2 vertical distributions simulated by the global CTM MOZART (Horowitz et al., 2003) and (3) the use of cloud parameters and surface albedo obtained from GOME measurements using the algorithms discussed by Koelemeijer et al. (2001) and Koelemeijer et al. (2003). A very similar method has been used to derive tropospheric NO_2 columns from SCIAMACHY measurements (Richter et al., 2005). Note that the use in the retrieval procedure of NO_2 vertical distributions simulated by MOZART (rather than CHIMERE itself) allows us to assume that the random part of uncertainties in NO_2 columns derived from satellite measurements and in those modelled by CHIMERE are statistically independent. This assumption is explicitly used in our inversion procedure. In this study, we use a combined set of NO_2 columns derived from GOME measurements and SCIAMACHY. We used GOME data because they are concurrent with EMEP data for near-surface concentrations of NO_2 available for summer 2001. The use of data for near-surface concentrations in parallel with the data for tropospheric column amounts is an important feature of our study. However, the horizontal resolution of GOME in west-east direction (about 300 km) is weak for our model grid (1/2 deg. resolution). Therefore, we used SCHIAMACHY data with a resolution of the model grid to deconvolute GOME data (as explained below). Unfortunately, EMEP and SCIAMACHY data were not available for the same year.

The idea of our method of deconvolution is to superimpose on the GOME data the fine spatial structure of some data of higher resolution. The deconvoluted GOME columns, $c_g^{(dc)}$, are defined as

$$c_g^{i(dc)} = \frac{c_h^i}{c_h^{i(\mathrm{conv})}} c_g^i, \tag{1}$$

where c_h are the data for NO_2 columns of higher spatial resolution, i is the index of a CHIMERE grid cell and

$$c_{h(i)}^{\mathrm{conv}} = \sum_{j=0}^{2m} c_{h(i-m+j)} \exp\left(-\frac{[j-m]^2}{m^2}\right) \tag{2}$$

are artificially convoluted high resolution data. This artificial convolution is intended to replicate the convolution of real NO_2 columns within the GOME window. Here, we approximate the shape of the GOME window on the longitudinal plane by the Gauss function with an efficient width m, which is assumed to be equal to three grid cells of CHIMERE. We assume also that a signal outside of the range of seven (i.e., $2m$+1) cells is negligible. A value of m is chosen as three, because then $2m$+1=7 corresponds to the approximate longitudinal resolution of GOME (7*0.5°≈280 km at 45° N). As the source of high-resolution data we could use either NO_2 columns derived from SCIAMACHY or those simulated by CHIMERE itself. The GOME data deconvoluted using NO_2 columns from SCIAMACHY are obviously preferable as they are more observationally based. The SCIAMACHY data that we use in this study have been retrieved from the measurements performed in 2004. We use the SCIAMACHY data for 2004 rather than for 2003 because the summer of 2003 was exceptionally hot, so that meteorological conditions of 2004 were likely to be more similar to those of 2001.

2.3 Comparison of measured and simulated data for NO_2 columns

Figure 2 presents distributions of tropospheric NO_2 columns derived from different sets of satellite data (GOME with different deconvolutions, SCIAMACHY), and also NO_2 columns from CHIMERE. It is seen that all these distributions are rather similar. CHIMERE gives slightly smaller values but this is mostly due to the fact that it does not take into account the upper troposphere. Strongly elevated magnitudes of NO_2 columns over Great Britain, Netherlands, Belgium, North-West of Germany, and the Ile-de-France region are seen both in observations and simulations. Figure 3 shows scatter plots with different versions of satellite data versus NO_2 columns from CHIMERE for each model grid cell, as well as scatter plots that allow comparing different sets of satellite data. The correlation between the modelled

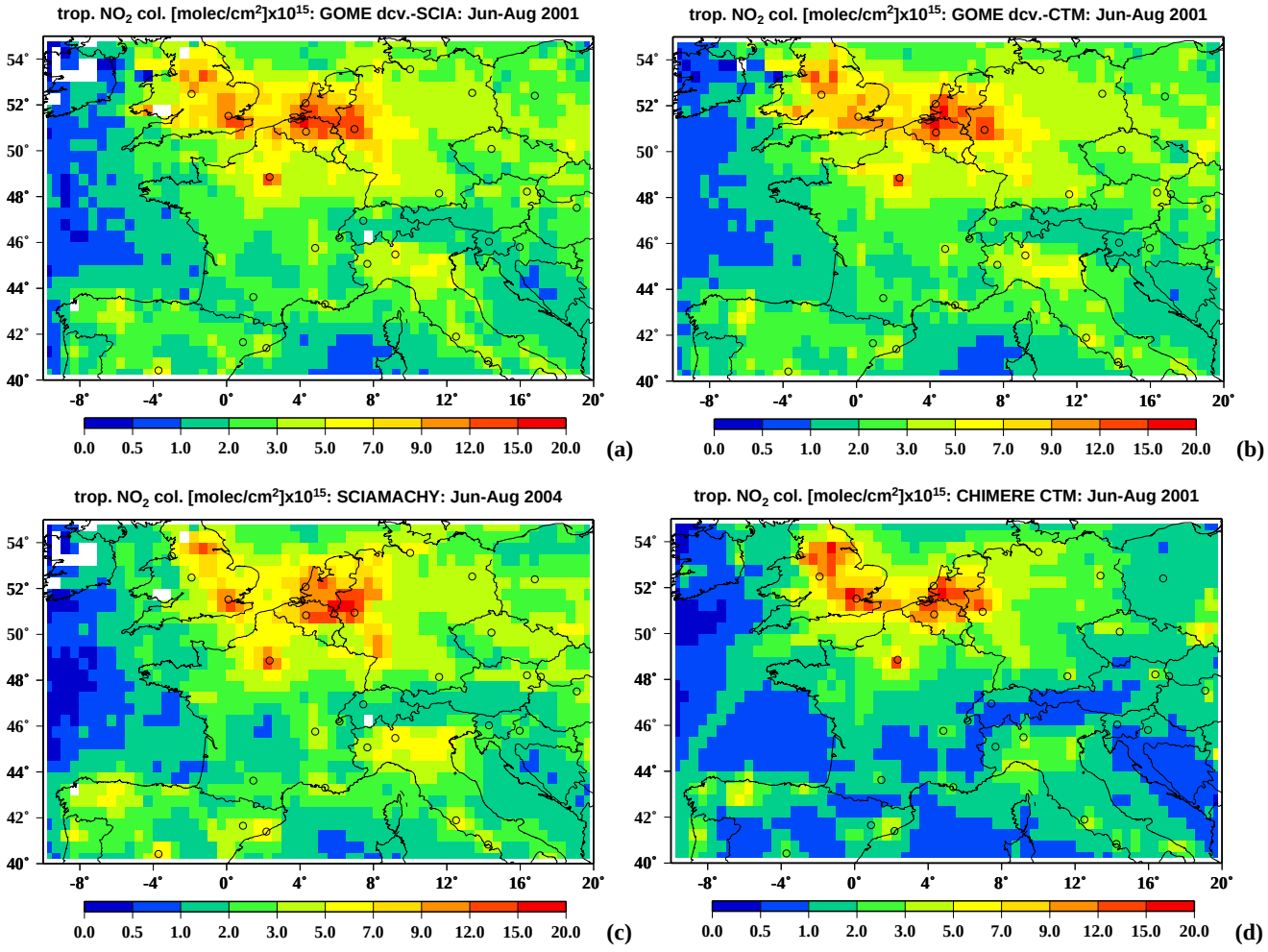

Fig. 2. Tropospheric NO_2 columns for different versions of satellite data in comparison with lower tropospheric NO_2 columns (below 500 hPa) calculated by CHIMERE. Blank areas designate the pixels for which the SCIAMACHY data have been missing.

and satellite data is rather high in all cases. It is noteworthy, however, that the distribution of points across the line of the linear fit is not quite symmetric. In particular, the data points corresponding to the largest range of magnitudes of NO_2 columns tend to be grouped on the upper side of the fit. This could be due to partial "blindness" of satellite instruments over highly polluted areas that could be caused by the presence of large amounts of aerosols.

The average values of the measured and simulated NO_2 columns are also given in Fig. 4. It is seen that systematic difference between them is about 8×10^{14} cm^{-2}. As it has been noted in Sect. 2.1, a considerable part of this bias may be due to omission of the upper troposphere in CHIMERE. If we admit that the mean column amount of NO_2 above 500 hPa pressure level is about 8×10^{14} m^{-2} (Konovalov et al., 2005), then the residuary part of the bias is about 10 percent. It remains unknown whether this bias is due to some systematic errors in the model, in emissions, or in the satellite data. Indeed, although several studies have already undertaken quantification of uncertainties in NO_2 columns derived from satellite measurements (e.g., Martin et al., 2003; Boersma et al., 2004; Heue et al., 2005), up to our knowledge there have yet been no publications characterizing uncertainties in satellite data in terms of random and systematic errors (in the spatial sense). Moreover, since different research groups performing retrieval of tropospheric NO_2 columns from satellite measurements employs different radiation models, it is probable that uncertainties for different sets of satellite data are also different. Possible uncertainties in NO_2 columns simulated by CHIMERE are also essentially unknown.

The correlation between GOME data deconvoluted using CHIMERE and NO_2 columns from CHIMERE itself is, as it should be expected, higher than in the case with GOME data deconvoluted with SCIAMACHY, but the difference in correlation is rather small. The agreement between different sets of satellite data is also rather good although not perfect. This is encouraging given the differences in the data sets (type of instrument, year, deconvolution procedure).

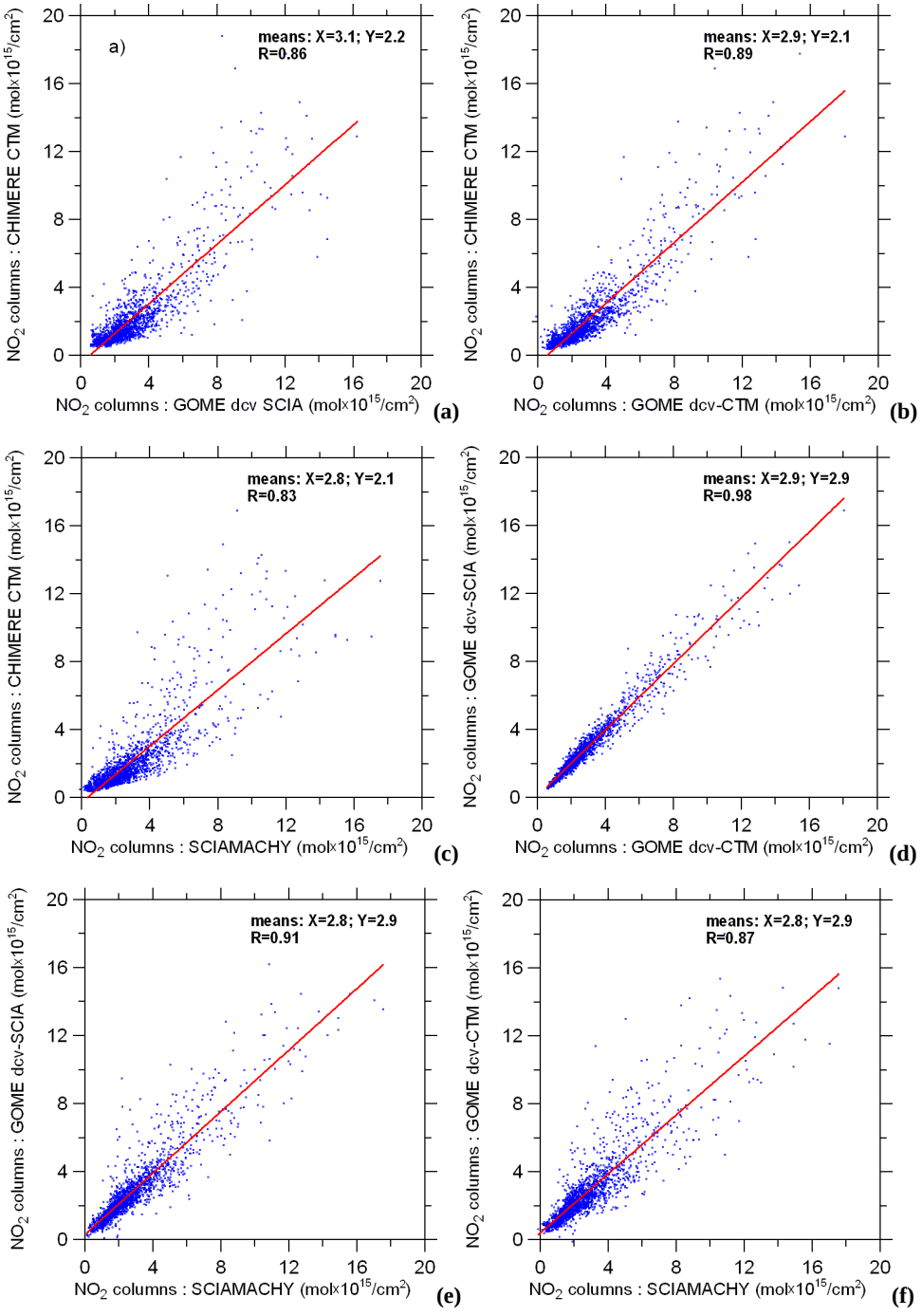

Fig. 3. Scatterplots of satellite and simulated data for NO_2 columns. Satellite data have been preliminarily projected to the CHIMERE grid. Each point represents one grid cell of the model.

2.4 The data of ground based measurements

We use data for near-surface NO_2 concentrations from the EMEP ground based monitoring network (http://www.nilu.no/projects/ccc/emepdata.html) for the year 2001. The locations of EMEP sites are shown in Fig. 4. This figure also presents the seasonally average concentrations measured by the EMEP stations in comparison with those simulated by CHIMERE. The important advantages of EMEP measurements are the common standards of quality control and that they are intended to reflect regional background conditions relatively unaffected by local emissions. The use of data

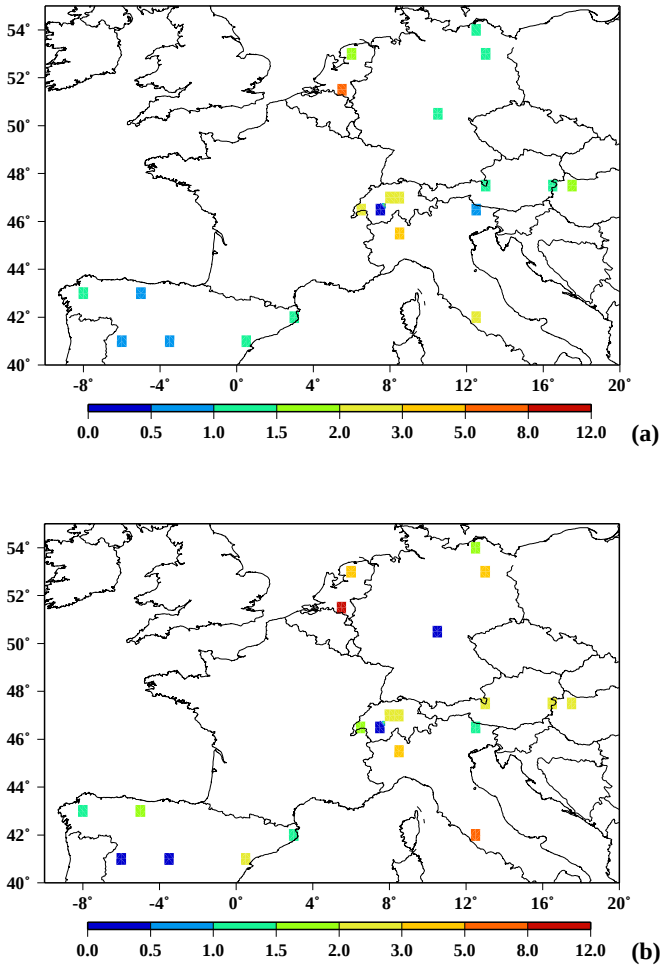

Fig. 4. **(a)** Observed EMEP and **(b)** modelled NO_2 concentrations ($\mu g/m^3$) averaged over three summer months (June–August) of 2001.

from several other monitoring networks (urban, regional, etc.) would pose serious methodological problems concerning criteria of data selection and treatment of uncertainties. However, an obvious disadvantage of the EMEP network is that it is rather sparse. In particular, data are missing entirely for France and Great Britain.

The differences between the modelled and observed data are, in general, rather large. In particular, the mean bias (observed minus modelled concentrations) and the mean absolute bias are found to be $-0.8\,\mu g/m^3$ and $1.1\,\mu g/m^3$, respectively, while the mean measured concentration is $1.9\,\mu g/m^3$. The differences between the modelled and measured concentrations are larger than a factor of 2 at 8 stations out of 21 considered. A significant part of all these discrepancies may be due to representativeness and measurement errors (Aas et al., 2000). NO_2 measurements are subject to interference with other nitrogen species, however the negative bias in observations (compared to the model) suggests that this is not a major problem. Large representativeness errors may be caused by insufficient resolution of the model's grid in case of such reactive species as NO_2 with spatially heterogeneous emission sources. Another part of discrepancies between the model and observations may be due to uncertainties of emissions. These uncertainties are discussed in Sect. 4. Note that based on comparison between measured and modelled data one station (out of 22 within the considered domain, for which data were available) situated in Poland (Sniezka, not shown) has been excluded from our analysis as an outlier: the concentration measured there was more than 6 times larger than the modelled one.

3 Inversion method

3.1 Problem definition

Let $\boldsymbol{E}$, $\boldsymbol{C}$ and $\boldsymbol{S}$ be vectors of the gridded anthropogenic NO_x emission rates, tropospheric NO_2 columns, and near surface concentrations of NO_2. While the true values of these characteristics are unknown, we have at our disposal the estimates of emission rates obtained from emission inventories $\boldsymbol{E}_a$, which will be referred to as the a priori emissions, as well as the tropospheric NO_2 columns derived from satellite measurements, $\boldsymbol{C}_o$, and the data of near surface concentrations, $\boldsymbol{S}_o$, for a limited number of sites. Using available estimates of emission rates, we can also evaluate NO_2 columns and near surface concentrations by means of a chemistry-transport model, which provides a functional relationships between emissions, columns, and concentrations, $\boldsymbol{C}_m(\boldsymbol{E})$ and $\boldsymbol{S}_m(\boldsymbol{E})$.

In the following, we consider the columns, concentrations and emissions averaged over three summer months. Besides, areas where anthropogenic emissions contribute less than a half to the tropospheric NO_2 column are excluded (calculated from the difference in a reference simulation and one with zero anthropogenic emissions). The excluded pixels (see Sect. 4) correspond mainly to sea areas, so in accordance to our calculations the tropospheric NO_2 column amounts over Western Europe are determined mostly by anthropogenic emissions (and only to a minor extent by biogenic emissions and advection across the boundaries).

The problem is to correct the a priori emissions using the observational data such that the a posteriori emissions would be closer to the true values than the a priori ones. We follow the probabilistic approach, which is commonly used in geophysical inverse modelling studies (see, e.g., Tarantola, 1987), including inverse modelling of sources of atmospheric trace gases (e.g., Enting, 2002). Accordingly, we treat all considered characteristics as random values which, however, satisfy certain restrictions. Specifically, we assume that their errors are multiplicative and satisfy lognormal probability distributions. We assume also that the errors in different grid cells are statistically independent and have the same standard deviations. In accordance to these assumptions, we can relate

the estimates and true values of the considered characteristics as follows,

$$\begin{aligned} \mathbf{e}_a &= \mathbf{e} + \Delta_e, \\ \mathbf{c}_o &= \mathbf{c} + \Delta_c, \\ \mathbf{s}_o &= \mathbf{s} + \Delta_s \end{aligned} \tag{3}$$

where **e**, **c** and **s** are natural logarithms of $\boldsymbol{E}$, $\boldsymbol{C}$ and $\boldsymbol{S}$, respectively, and errors Δ_e, Δ_c, and Δ_s satisfy the normal distribution with non-zero means in the general case.

The assumption regarding the multiplicative character of errors seems to be appropriate in case of emissions because the standard methods used for evaluations of emissions involve multiplying several different factors, each of which may contribute to the total uncertainty of emission inventory data (see, e.g., Kühlwein and Friedrich, 2000). Our previous analysis (Konovalov et al., 2005) has shown that the uncertainties in tropospheric NO_2 columns derived from GOME measurements and calculated by a CTM for Western Europe are also predominantly of multiplicative character. The lognormal distribution for errors appears to be the optimal choice in a case of strictly positive physical characteristics (Mosegaard and Tarantola, 2002). The use of the lognormal distribution is especially justified in our study due to large relative uncertainties of NO_2 columns and NO_x emissions.

3.2 Overview of the inverse modelling scheme

Our method is discussed in detail in the next sections. Here, we provide a brief overview of its key features. The basic principle of our method is similar to that used in many recent atmospheric inverse modelling studies. It includes the equations defining optimal (maximum likelihood) a posteriori estimate for emissions as a function of measurement data, a priori emission estimates and several parameters describing uncertainties in a model, in measurements and in a priori emissions. As already noted in the Introduction, the most important distinctive feature of our method is that the uncertainty parameters are defined in the framework of the inversion procedure self-consistently. In other words, these uncertainties are internal, rather than external parameters of our inversion scheme. The estimation of uncertainties (quantified in terms of the respective standard deviations) proceeds in several steps. First, we utilize ground-based observations of near surface NO_2 concentrations in attempt to find the ratio of optimal estimates of the standard deviations of the columns and emissions. The idea is that the emission rates, which are obtained using the most reliable uncertainty estimates, are expected to provide the best agreement of the model output with the ground-based data. In parallel, we use the variance of the difference between the measured and simulated NO_2 columns as an estimate of the upper limit of total random uncertainties in NO_2 columns. We employ also a modelled relationship between uncertainties in NO_x emissions and respective uncertainties in NO_2 columns for separating a part of uncertainties in NO_2 columns due to uncertainties in emissions. As a result, we obtain estimates of the standard deviation of NO_2 columns (which characterises the total uncertainty in NO_2 columns due to both errors in the model and in measurement data), and the standard deviation of a priori emissions. We obtain then the maximum likelihood estimates for the a posteriori emissions taking into account the estimated magnitudes of the uncertainty parameters. The a posteriori estimates are uncertain to some degree due to uncertainties in measured data and model errors, but also due to uncertainties in our estimates of the standard deviations of NO_2 columns and a priori emissions.

We estimate the uncertainties in our results by means of a special Monte-Carlo experiment. This experiment involves generating a number of synthetic datasets of tropospheric NO_2 columns, near surface NO_2 concentrations and NO_x emissions with randomly sampled errors and analysing the differences between the a posteriori estimates obtained with synthetic and real data. The Monte Carlo experiment provides some more information on the statistical properties of our estimates and this information is used to improve the estimates.

Another important aspect of our method is to find an approximation for the modelled relationship between NO_x emissions and NO_2 columns and concentrations. To this purpose, we take advantage of the relatively short transport distance of freshly emitted NO_x in the lower atmosphere due to the relatively short lifetime of NO_x during summer. This drastically reduces the computational demand and allows the practical realisation of our method.

3.3 Maximum likelihood estimates

3.3.1 Basic formulations

In accordance to Bayes's theorem and the assumptions regarding the statistical properties of the errors, which have been formulated in Sect. 3.1, we have the following conditional probability distribution function (*pdf*) for the logarithms of the a posteriori emission rates:

$$p(\mathbf{e}\,|\mathbf{c}_o) \propto \exp\left\{-\sum_{i=1}^{N}\left[\frac{(c_o^i - c_m^i(\mathbf{e}) - \delta_c^i)^2}{2\sigma_c^2} + \frac{(e^i - e_a^i)^2}{2\sigma_e^2}\right]\right\}, \tag{4}$$

where N is the total number of grid cells, σ_c and σ_e are the the uncertainties (in terms of standard deviations) of logarithms of NO_2 columns and NO_x emissions, and δ_c is the difference between the mathematical expectations of $\mathbf{c}_0$ and $\mathbf{c}_m$, or, in other words, it is the difference between their systematic errors. We assume that it may depend on the magnitude of NO_2 columns in a given grid cell. The evaluation of δ_c is discussed below in the next section.

The variance σ_c^2 represents here both the model and measurement errors and is equal to the sum of the variances of

errors of the model and the observations taken separately (see, e.g., Tarantola, 1987; Enting, 2002). By subtracting δ_c defined as the difference between the mathematical expectations of $\mathbf{c}_0$ and $\mathbf{c}_m$ we accept that our method does not correct any systematic errors in a priori emissions. The correction of systematic errors is not possible, because, as noted above, it is impossible to know to which extent to attribute δ_c either to systematic errors in emissions, in the model and in observations. Accordingly, in this study we try to estimate and correct only the random part (in the spatial sense) of the uncertainties in the a priori emissions, and the standard deviations σ_c and σ_e represent here only the random parts of the uncertainties in the respective characteristics. When σ_c, σ_e and δ_c are known, the distribution $p(\mathbf{e}|\mathbf{c}_0)$ (Eq. 4) provides the complete solution of the inverse problem. But in practice, it is much more convenient to deal with the results of inverse modeling expressed in terms of a posteriori estimates and their uncertainties, rather than statistical distributions. Our analysis is based on the maximum-likelihood estimate $\hat{\mathbf{e}}$, which provides the minimum of the function

$$G(\mathbf{e}) = \sum_{i=1}^{N} \left[\frac{(c_o^i - c_m^i(\mathbf{e}) - \delta_c^i)^2}{2\sigma_c^2} + \frac{(e^i - e_a^i)^2}{2\sigma_e^2} \right] \quad (5)$$

and satisfies to the following set of equations:

$$\sum_{i=1}^{N} \left[(c_o^i - c_m^i(\hat{\mathbf{e}}) - \delta_c^i) \frac{\partial c_m^i(\hat{\mathbf{e}})}{\partial \mathbf{e}^j} \right] + \varphi^2(\hat{\mathbf{e}}^j - e_a^j) = 0, \quad j = 1, \ldots, N. \quad (6)$$

It is important to note that $\hat{\mathbf{e}}$ does not depend separately on σ_c and σ_e, but only on their ratio,

$$\varphi = \frac{\sigma_c}{\sigma_e}. \quad (7)$$

Unlike most other inverse modelling studies, we do not assign values to the error variances "by definition", because in our case they are essentially unknown. Rather, we consider them as random variables and try to obtain their optimal estimates by using available measurements. The main idea is to consider first $\hat{\mathbf{e}}$ as a function of φ and to optimise the latter by comparing model results with independent observations. In this study, we employ surface measurements of NO_2 as a source of independent observational information. We expect that the best estimate for φ should yield the best agreement between the observed and modelled data for surface concentrations of NO_2. Formally, we can assign the conditional *pdf* for φ using Bayes's theorem:

$$p(\varphi\,|\mathbf{s}_o) \propto \exp\left\{ -\sum_{i=1}^{L} \left[\frac{(s_o^i - s_m^i\left(\hat{\mathbf{e}}[\varphi]\right) - \delta_s^i)^2}{2\sigma_s^2} \right] \right\} p_a(\varphi), \quad (8)$$

where $\mathbf{s}_0$ and $\mathbf{s}_m$ are observed and modelled NO_2 concentrations, δ_s is the difference between their systematic errors, σ_s^2 is the total variance of the random errors, L is a number of stations considered, and $p_a(\varphi)$ is the a priori *pdf* for φ, which reflects our a priori knowledge on the value of φ. Ideally, it would be reasonable to assume that $p_a(\varphi)$ is homogeneous. This option would reflect the lack of a priori knowledge about the true value of φ. However, in order to obtain a numerical solution of the problem, we assume that φ is distributed uniformly within a very broad but nevertheless limited interval [0.01, 10] and cannot take any value outside of this interval.

The maximum-likelihood estimate of φ, which is denoted below as $\hat{\varphi}$, can be obtained after resolving the following minimization problem which has to be solved together with the Eqs. (6):

$$J(\hat{\varphi}) = \min\{J(\varphi)\};$$
$$J(\varphi) = \sum_{i=1}^{L} \left[(s_o^i - s_m^i\left(\hat{\mathbf{e}}[\varphi]\right) - \delta_s^i)^2 \right]. \quad (9)$$

It is noteworthy that $\hat{\varphi}$ does not depend on the unknown σ_s^2. As a result, we obtain the optimal a posteriori estimates $\hat{\mathbf{e}}(\hat{\varphi})$ under the given values of observed NO_2 columns and concentrations.

3.3.2 Evaluation of the systematic errors

We represent the difference between systematic errors of NO_2 columns calculated by CHIMERE and those derived from satellite measurements as a function of magnitude of the measured columns using a running window technique. This approach allows us, in particular, to take into account differences in the systematic biases of NO_2 columns for more and less polluted regions (see Sect. 2.3). Specifically, we arrange the measured NO_2 columns in ascending order and evaluate δ_c as the average difference between measured and modeled NO_2 columns within the "window":

$$\delta_c^i \cong \frac{1}{N_w^i} \sum_{j=1}^{N_w^i} \left(c_o^{i(j)} - c_m^{i(j)}(\mathbf{e}_a) \right), \quad (10)$$

where N_w is the number of data points in the window. This number should be sufficiently large, so that uncertainties in estimates of δ_c due to random errors would be much smaller than the random errors themselves, and yet it should be sufficiently small so that the existing differences in systematic errors for different magnitudes of NO_2 columns would not be suppressed by averaging. We have defined N_w for each grid cell separately based on the simple criterion that maximum relative changes of magnitudes NO_2 columns inside a window should not exceed 50%. On the average, the windows include about 300 data points. The results of inversions proved to be rather insensitive to the choice of window parameters as long as they satisfy to the qualitative criteria outlined above. As it already has been noted in Sect. 2.3, a significant part of systematic differences between the modeled

and simulated NO_2 columns is due to omission of the upper troposphere in CHIMERE. This limitation of our model is reflected also in magnitudes of the differences δ_c. The mean of absolute values of δ_c calculated with original data from CHIMERE is 0.4, but it drops to 0.2 when the estimated upper tropospheric NO_2 (5×10^{14} cm^{-2}) is taken into account.

The difference in systematic errors of measured and modelled NO_2 concentrations is estimated in a similar way as above for NO_2 columns. The only difference is that because of the limited statistics we disregard a possible dependence of this error on the magnitudes of measured concentrations. Accordingly, we have:

$$\delta_s \cong \frac{1}{L}\sum_{i=1}^{L}\left(s_o^i - s_m^i(\mathbf{e}_a)\right). \quad (11)$$

This difference is -0.1.

3.3.3 Model approximation

Finding the exact solution of the problem defined by Eqs. (6) and (9) by means of iterative numerical methods of the nonlinear optimization would be computationally extremely expensive, even if we used the adjoint model approach. Instead, we use an original approach that reduces the computational demand and allows us to find an approximate but yet sufficiently accurate solutions. The idea is to simplify the calculation of the modeled relationships between NO_x emissions and NO_2 columns or concentrations by substituting the original model by a set of linear relations describing the considered relationships approximately. We take into account that the typical range of transport of freshly emitted NO_x is rather limited. Accordingly, our statistical models are defined (in the case of the columns) as follows:

$$C_i(\boldsymbol{E}) := C_i(\boldsymbol{E}_a)\left(1+\sum_{j=1}^{(2M+1)^2}\alpha_j^i(E_j^i - E_{aj}^i)/E_{aj}^i\right), \quad (12)$$

where α_j^i are regression coefficients, which represent the sensitivity of the NO_2 column in the grid cell i to a perturbation of emission rate in the grid cell j, and M is the number of layers of grid cells around the "central" cell i: the larger is M, the more distant transport of NO_x is taken into account. Because the CHIMERE grid has a constant resolution of 0.5°, the actual distance of transport, which is taken into account, depends on latitude and direction. For the reference, one degree of latitude corresponds to about 111 km, while one degree of longitude varies from 85 km in South of the domain to 65 km in North. The statistical models are built using results of a sufficiently large number of model runs with pre-specified small random perturbations of emissions in each of the model grid cells. Accordingly, the coefficients α_j^i are obtained by solving a set of linear equations for relative perturbations of emissions and corresponding responses of NO_2 columns. Technically, the respective equations are solved using the SVD (Singular Value Decomposition) method (Press et al., 1992). Similar models are built for the relationships between NO_x emissions and near-surface concentrations. While our statistical models are formulated initially in terms of relative perturbations of NO_x emissions and NO_2 columns, we have to reformulate them for the logarithmic variables:

$$c_i(\mathbf{e}) := c_i(\mathbf{e}_a) + \ln\left(1+\sum_{j=1}^{(2M+1)^2}\alpha_j^i\left[\exp(e_j^i - e_{aj}^i) - 1\right]\right), \quad i = 1, ..., N. \quad (13)$$

The optimal number of "random" model runs depends on the desired accuracy, the effective distance of transport, and the nonlinearities in the real relationships between emissions and columns, but, importantly, it does not depend on the total number of grid cells as soon the dimensions of the model domain exceed the typical range of NO_2 transport. In situations relevant for this study, the performance of the statistical models has been found to improve gradually as the number of forward runs of an original CTM with randomly perturbed emissions is increased but reaches saturation when this number approaches 100. Accordingly, all the results discussed below have been obtained with the number of CHIMERE runs equal 100. Note that although this number is not small, it is, nevertheless much smaller than the number of the emission parameters to be optimised (∼1600 in this study), and, therefore, our method is very beneficial in terms of the computational demand when compared with the direct variational approach. The optimal choice of a value of the parameter M is discussed in Sect. 3.3.4. The results presented below have been obtained with M equal 2, unless another value is indicated.

Note finally that although we use linear models, it would be possible to built similar nonlinear statistical models, such as, for example, nonlinear regressions based on neural networks (e.g., Gardner and Dorling, 1998; Hornik et al., 1989; Konovalov, 2002). The use of nonlinear models would enable reducing the uncertainties but at the expense of a larger computational cost.

3.3.4 Numerical scheme

The solution of the problem defined by Eqs. (6) and (9) is found using standard numerical methods (Press et al., 1992). Specifically, making some random initial guess for a value of φ, we minimise the function $G(\mathbf{e})$ (see Eq. 5) iteratively by means of the steepest descent method using the a priori emissions as initial guess. Although the steepest descent method is not optimal in terms of computational demand, it has been chosen because of its robustness and stability. The evaluation of partial derivatives of $G(\mathbf{e})$ with respect to e_i at each

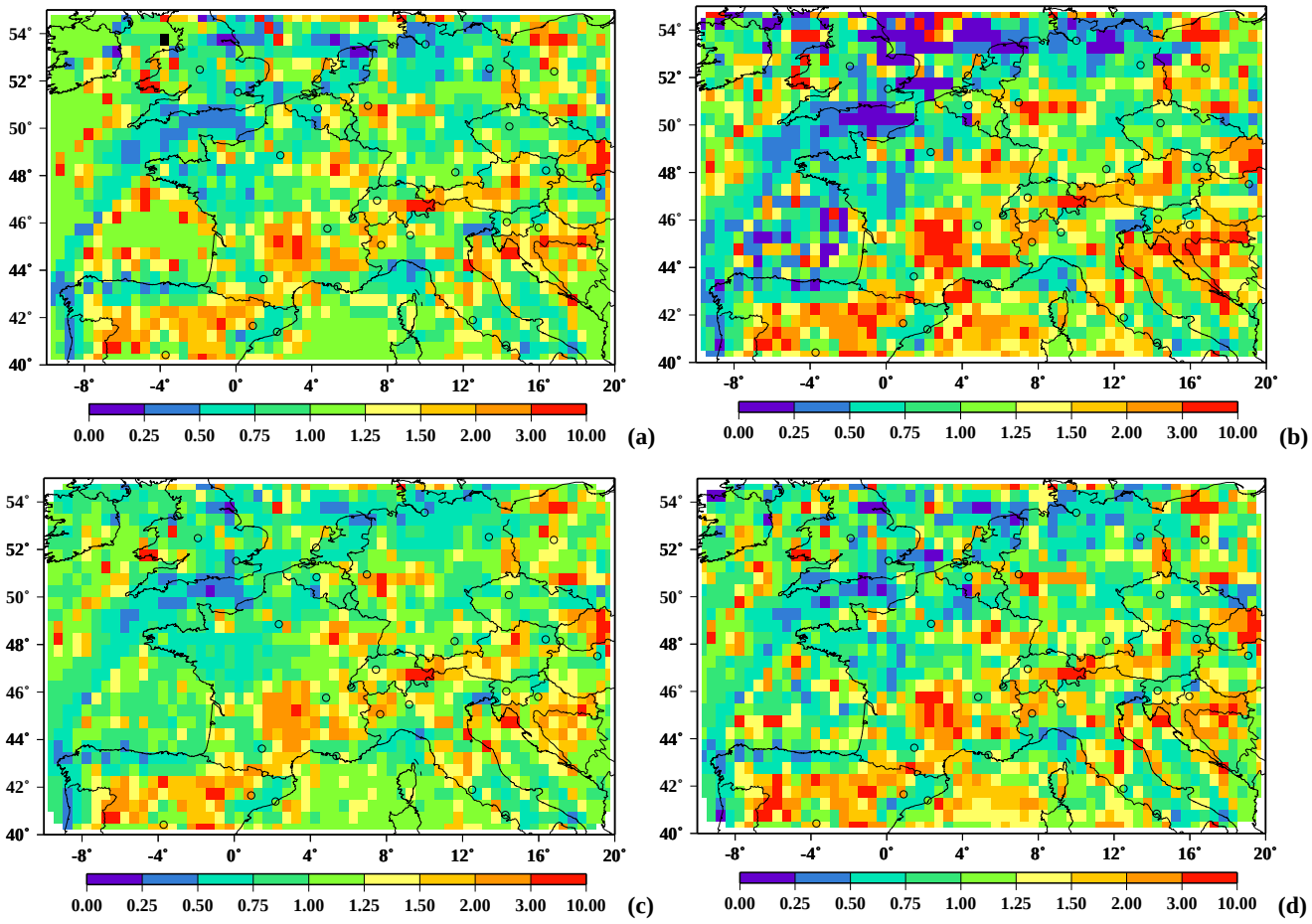

Fig. 5. Tests of the inversion scheme: **(a)** the target and **(b–d)** retrieved ratios between perturbed and a priori NO_x emissions. The retrievals are performed with the parameter M equal to (b) 1, (c) 2 and (d) 3. M is the number of CHIMERE grid cells corresponding to the maximum distance of NO_x transport taken into account in the linearized models (see Eq. 12).

iteration involves, in particular, the derivatives of $c_j(\mathbf{e})$ with respect to e_i that are estimated using the linear approximation (13). As soon as the minimum of $G(\mathbf{e})$ is reached, we evaluate the function $J(\varphi)$ (see Eq. 9) and correct a value of φ using the golden section search method. The whole procedure is repeated iteratively until the minimum of $J(\varphi)$ is reached.

3.3.5 Test cases

The main objective of the tests described in this section is to examine the performance of our inversion procedure described above. The idea of the tests is to perform inversions for synthetic data and to compare the results with the known exact solution. The synthetic NO_2 data were created using CHIMERE with perturbed a priori emissions. Taking into account that the accuracy of inverse modelling results may depend on the magnitude and spatial distribution of uncertainties of the a priori emissions and the observation data, the test cases considered below have been created after having applied the procedure to the real data. Specifically, in order to best represent real conditions, we assigned the perturbations of the a priori emissions using the a posteriori emissions found with real data (Sect. 4). The ratios between the a posteriori and a priori emissions have been scaled so that the standard deviation of the natural logarithms of emission perturbations was 0.6 (this is a dimensionless quantity). This value is representative of our estimate for the standard deviation for the uncertainties in the a priori emissions (see Sect. 4). These emission perturbations are shown in Fig. 5, which presents also the results of the inversion performed with different values of M (1, 2 and 3) in the models (12). It is seen that the retrieved emissions capture the main features of the target in all cases shown, although there are also noticeable differences. The results obtained with M equal 1 and 3 are evidently least and most accurate, respectively.

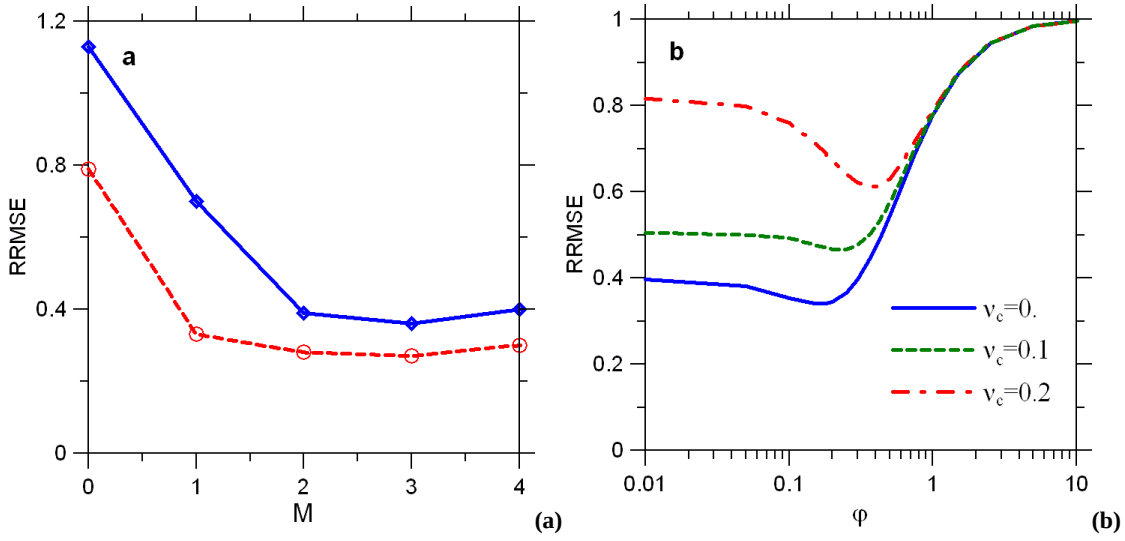

Fig. 6. The root relative mean square error (RRMSE) calculated with synthetic data for NO_2 columns as a function of the parameters **(a)** M and **(b)** φ. M is the number of CHIMERE grid cells corresponding to the maximum distance of NO_x transport taken into account in the liberalized models (see Eq. 12), and φ is the ratio of the presumed uncertainties (standard deviations) in the logarithms of NO_2 columns and a priori emissions (see Eqs. 4 and 7). The solid and dashed lines in the plot (a) have been obtained with perfect ("no noise") data under φ=0 and represent RRMSE expressed in terms of logarithmic and absolute emission rates, respectively. Different curves in the plot (b) have been obtained with M equal 2 and correspond to different levels of noise (ν_c) added to the logarithms of NO_2 columns.

In order to quantify the uncertainty of retrievals we consider the root relative mean squared error (RRMSE),

$$\mathrm{RRMSE} = \left[\frac{\sum_i \left(\hat{e}^i(\varphi) - e_t^i\right)^2}{\sum_i \left(e_a^i - e_t^i\right)^2} \right]^{1/2}, \qquad (14)$$

where $\mathbf{e}_a$, $\mathbf{e}_t$, and $\hat{\mathbf{e}}(\varphi)$ are initial (unperturbed), target, and retrieved values of logarithms of NO_x emissions, respectively. A similar statistics has been defined for the absolute values of emisions ($\boldsymbol{E}$). Some results are presented in Fig. 6. It is seen, in particular, that the RRMSE for logarithms of emissions decreases strongly as M increases from 0 to 2 (see Fig. 6a). The case with M equal to zero corresponds to the assumption of a direct local relationship between NO_x emissions and NO_2 columns in a given grid cell, whereas in other cases the NO_x transport between the $(2M+1)^2$ closest grid cells is taken into account. Therefore, this result demonstrates the importance of the transport in our inverse modelling problem. The RRMSE (14) expressed in terms of absolute emissions (that is, after substituting logarithms of emission rates for their absolute values) gives more weight to regions more strongly polluted. This statistics drops more rapidly to a small value of RRMSE (already for M=1), since the NO_2 columns over regions with large emissions are determined mostly by their nearby sources. While the RRMSE reaches a minimum under M equal 3, it is only very insignificantly larger when M equals 2. Since the computational costs proved to be much smaller with M equal 2, we use this value throughout this study. Deteriorating quality of the inversion in the case with M equal 4 is, probably, due to the fact that in this case the number of grid cells in the sub-domain of the statistical model (81) is close to the number of "random" model runs (100), so that the information provided by these runs becomes insufficient for fixing the coefficients of the statistical models.

While the results presented in Fig. 6a have been obtained fixing a zero value of φ (no a priori information on emissions has been used), the inversions performed with non-zero φ can be more accurate as it is evidenced by results shown in Fig. 6b. This figure presents the dependence of RRMSE (for logarithmic variables) on φ for case of M=2 and without uncertainty in observations (as in Fig. 6a), but also for two more realistic cases when the available data for NO_2 columns are to some degree uncertain. The errors of logarithms of the columns have been sampled from the normal distribution with zero mean and the standard deviation equal to either 0.1 or 0.2. In accordance to the results discussed in Sect. 4, the uncertainty in real data is most likely to be about 20%, although this estimate is very uncertain. It is seen that the use of non-zero value of φ enables improvement of the retrievals even for the ideal case with no noise in the data. This improvement merely reflects the obvious fact that the model approximation (12) is not perfect. It is seen also that in accordance with our tests, the uncertainty in a priori emissions could be reduced almost up to 3 times if the data were perfect, while the maximum reduction of uncertainty for the case with 20% of noise in the data is about 40%. Note that

the last result is consistent with the results obtained with real data (see Sect. 4).

We can conclude that our approximate method is capable of reducing uncertainties in a priori emission to a large extent. However, the actual improvement of the a priori emission estimates is likely to be limited by uncertainties in the measured and simulated data for NO_2 columns. The test results also emphasize the importance of a proper choice of the value of φ, especially when the uncertainty in input data is significant.

3.4 Estimation of uncertainties

3.4.1 Evaluation of the standard deviations of the input data

Values for the standard deviations of uncertainties in NO_2 columns (σ_c) and NO_x emissions (σ_e) are needed in order to estimate uncertainty in the a posteriori solution and, besides, they are interesting in themselves for characterizing uncertainties in measurement data and emissions prescribed in the model. The standard deviations σ_c and σ_e under a given value of their ratio φ (Eq. 7) are evaluated as follows. We assume (i) that the random uncertainties in NO_2 columns derived from satellite measurements (c_0) and those in the NO_2 columns simulated by CHIMERE (c_m) are statistically independent, and (ii) that the parts of the differences between the measured and modeled NO_2 columns due to uncertainties in the a priori emissions and other kinds of errors are statistically independent. Accordingly, we have:

$$\frac{1}{N}\sum_{i=1}^{N}\left(c_o^i - c_m^i(\mathbf{e}_a) - \delta_c^i\right)^2 + \Delta_{\text{apr}}^2 \cong \sigma_c^2 + \frac{1}{N}\sum_{i=1}^{N}\left(c_m^i(\mathbf{e}_t) - c_m^i(\mathbf{e}_a)\right)^2, \quad (15)$$

where $\mathbf{e}_t$ are the unknown true emission rates, Δ_{apr} is the misfit of NO_2 columns calculated by the statistical models (13). The first term in the left-hand part of Eq. (15) approximates the variance of total random uncertainties in both NO_2 columns derived from satellite measurements and in NO_2 columns calculated by CHIMERE with the a priori NO_x emissions (see a discussion of this approximation in more detail in Sect. 6.1 of our earlier paper (Konovalov et al., 2005)). If we knew values of true emissions, then we could find σ_c directly from Eq. (15) and then estimate σ_e using Eq. (7). However, since we do not know the true emissions, we have to substitute them for some surrogate values. In order to provide a reliable estimate of the last term in the left-hand part of the Eq. (15), these surrogate emissions should satisfy to the following obvious conditions. First, the differences between the natural logarithms of the surrogate and a priori emissions should have the variance equal to σ_e^2 (that is, the same as the variance of the differences between the natural logarithms of the true and a priori emissions). And second, the spatial structure of the differences between the logarithms of the surrogate and a priori emissions should be similar to the spatial structure of the differences between the logarithms of the true and a priori emissions. Taking into account that the best available estimates of the true emissions are the a posteriori estimates $\hat{\mathbf{e}}$, we define the surrogate emissions, $\mathbf{e}_s$, as follows:

$$\mathbf{e}_s = \frac{\sigma_e(\hat{\mathbf{e}} - \mathbf{e}_a)N^{1/2}}{\left[\sum_{i=1}^{N}\left(\hat{e}^i - e_a^i\right)^2\right]^{1/2}} + \mathbf{e}_a, \quad (16)$$

Such combination of the a posteriori and a priori emissions allows us to satisfy both conditions. Then, using the definition of φ (Eq. 7), we can rewrite Eq. (15) as follows:

$$\frac{1}{N}\sum_{i=1}^{N}\left(c_o^i - c_m^i(\mathbf{e}_a) - \delta_c^i\right)^2 + \Delta_{\text{apr}}^2 \cong \varphi^2\sigma_e^2 + \frac{1}{N}\sum_{i=1}^{N}\left(c_m^i(\mathbf{e}_s[\sigma_e]) - c_m^i(\mathbf{e}_a)\right)^2 \quad (17)$$

This equation involves only one unknown variable σ_e and can be solved iteratively. A value of Δ_{apr}^2 has been estimated by means of the test with the synthetic dataset described in the previous section. It is found to be about 0.01. This value, which has been used throughout this study, is much smaller than a value of the first term in the left-hand side of Eq. (15), which, in our case, is about 0.18.

The uncertainty (in terms of the standard deviation) in near-surface concentrations of NO_2, σ_s, is estimated as follows:

$$\sigma_s^2 \cong \frac{1}{L}\sum_{i=1}^{L}(s_o^i - s_m^i(\mathbf{e}_a) - \delta_s)^2. \quad (18)$$

The value found for σ_s is 0.63. Similar to σ_c, σ_s represents in fact a combination of the measurement and simulation error of near surface NO_2. This estimate is less certain than estimates of σ_c and σ_e, because the number of data points for near-surface concentrations is rather limited (about 20). However, as soon as $\mathbf{e}_a$ is different from $\mathbf{e}_t$, a value of σ_s given by Eq. (18) is more likely to be overestimated than underestimated, because it includes not only uncertainties in the model and measurement data, but also the errors due to uncertainties in emissions. From a practical point of view, an overestimation of uncertainties in results is preferable to an underestimation.

3.4.2 Monte Carlo experiment

While the formulations presented in Sect. 3.3 constitute the core of our inversion scheme, the complete solution of the inverse problem requires not only finding optimal a posteriori estimates but also their uncertainties. The evaluation of uncertainties in any estimate could be rather straightforward, if we had an explicit expression for the a posteriori *pdf*. In such a case we could use any Monte Carlo algorithm, e.g.,

the Metropolis's one (Metropolis et al., 1953), that enables sampling from a given multi-dimensional distribution. Our situation, however, is much complicated by the fact that we do not have an explicit expression for the a posteriori distribution of emissions, since standard deviations in the statistical distribution defined by Eq. (4) are also considered as random values satisfying to some unknown *pdf*. Thus, we have to use another method, which, nevertheless, is also based on the Monte Carlo approach.

The idea of the method employed here is described, e.g., in Press et al. (1992). Briefly, we use the uncertain measurement data as a surrogate for the true data and generate a number of sets of synthetic data based on our best understanding of the character of uncertainties in real data. These synthetic data are assumed to be equivalent (in a statistical sense) to the real measurement data and are employed to obtain a set of the maximum-likelihood estimates of emissions, which are used further to draw the conclusion about the uncertainty of the best estimate. As the best a posteriori estimate, we consider here the maximum likelihood estimate obtained for a selected value of φ which is defined as the median of the range of values obtained from the Monte Carlo experiment. The a posteriori emissions obtained for a median value of φ have been found to be less uncertain (based on results of the Monte Carlo experiment) than in the case with the maximum likelihood estimate of φ.

More in detail, our Monte Carlo procedure includes the following steps.

1. Prescribe the a priori values for the standard deviations for columns and emissions, σ_c and σ_e. We assume initially that the a priori value of σ_c is homogeneously distributed within the broad interval constrained by the mean squared difference between the modelled and measured NO_2 columns, that is:

$$\sigma_c \in \left[0; \left\{\frac{1}{N}\sum_{i=1}^{N}\left(c_o^i - c_m^i(\mathbf{e}_a) - \delta_c^i\right)^2 + \Delta_{\text{apr}}^2\right\}^{1/2}\right] \quad (19)$$

   The corresponding value of σ_e is then evaluated using the Eq. (17) (in which the term $\varphi^2\sigma_e^2$ is replaced with σ_c^2) together with the Eq. (16) involving the maximum likelihood estimates for emissions obtained using the real data for NO_2 columns and concentrations (see Sects. 3.3.1–3.3.4).

2. Define sets of synthetic data for the a priori emissions, NO_2 columns and concentrations:

$$\begin{aligned}\mathbf{e}_a &:= \mathbf{e}_a + \Delta_e,\\ \mathbf{c}_o &:= \mathbf{c}_o + \Delta_c,\\ \mathbf{s}_o &:= \mathbf{s}_o + \Delta_s,\end{aligned} \quad (20)$$

   where Δ_e, Δ_c, and Δ_s are random numbers sampled from the normal distribution.

3. Find the maximum likelihood estimate for φ as the joint solution of the set of the Eqs. (6) and the minimization problem (9) using the synthetic data (20).

4. Re-estimate σ_c and σ_e with φ found in the previous step. These new estimates are now constrained by ground-based measurements and thus they should be more certain than the a priori estimates prescribed at the first step.

5. Repeat the steps (2) and (3) using these new estimates for σ_e and σ_c and, as a result, find the maximum likelihood estimates for φ as well as for the NO_x emissions. This step is the core of our Monte Carlo experiment.

6. Define the best a posteriori estimate φ_p as the median of all optimal φ from the current and previous iterations; find the best a posteriori estimate for emissions, $\mathbf{e}_p$, as well as for σ_e and σ_c as the solutions of Eqs. (6) and (17) under $\varphi{=}\varphi_p$.

7. Calculate the confidence intervals for $\mathbf{e}_p$ and for the best estimates of σ_e and σ_c that include at least 68.3% of their closest maximum likelihood estimates from different iterations.

These steps are performed iteratively until the convergence of all the estimates is reached. The results presented below have been obtained after 300 iterations.

4 Results

4.1 A posteriori emissions and uncertainty statistics

Figure 7 presents the a priori and a posteriori estimates for total (biogenic plus anthropogenic) emissions and the ratio of logarithms of these estimates. Because we did not optimise the biogenic emissions, their uncertainties may contribute to the difference between the a posteriori and a priori anthropogenic emissions. Therefore, it is indeed best to present the results in terms of total NO_x emissions, rather than only their anthropogenic part. The a posteriori emissions shown in Fig. 7 have been obtained using GOME data deconvoluted with NO_2 columns from SCIAMACHY. We consider the results obtained with this set of satellite data as the most reliable, and this set is referred below as "standard". However, in order to get an idea of the robustness of our results, we present also the a posteriori emissions obtained with alternative datasets (see Fig. 8). In the case of GOME data deconvoluted using CHIMERE, our procedure may give incorrect results because these data are obviously not fully independent of our model. As to SCIAMACHY data, they do not correspond to the same year as input parameters of the model and the data of ground based measurement and, accordingly, they have been found to be more uncertain (in the sense that they contain less retrievable information on NO_x emissions

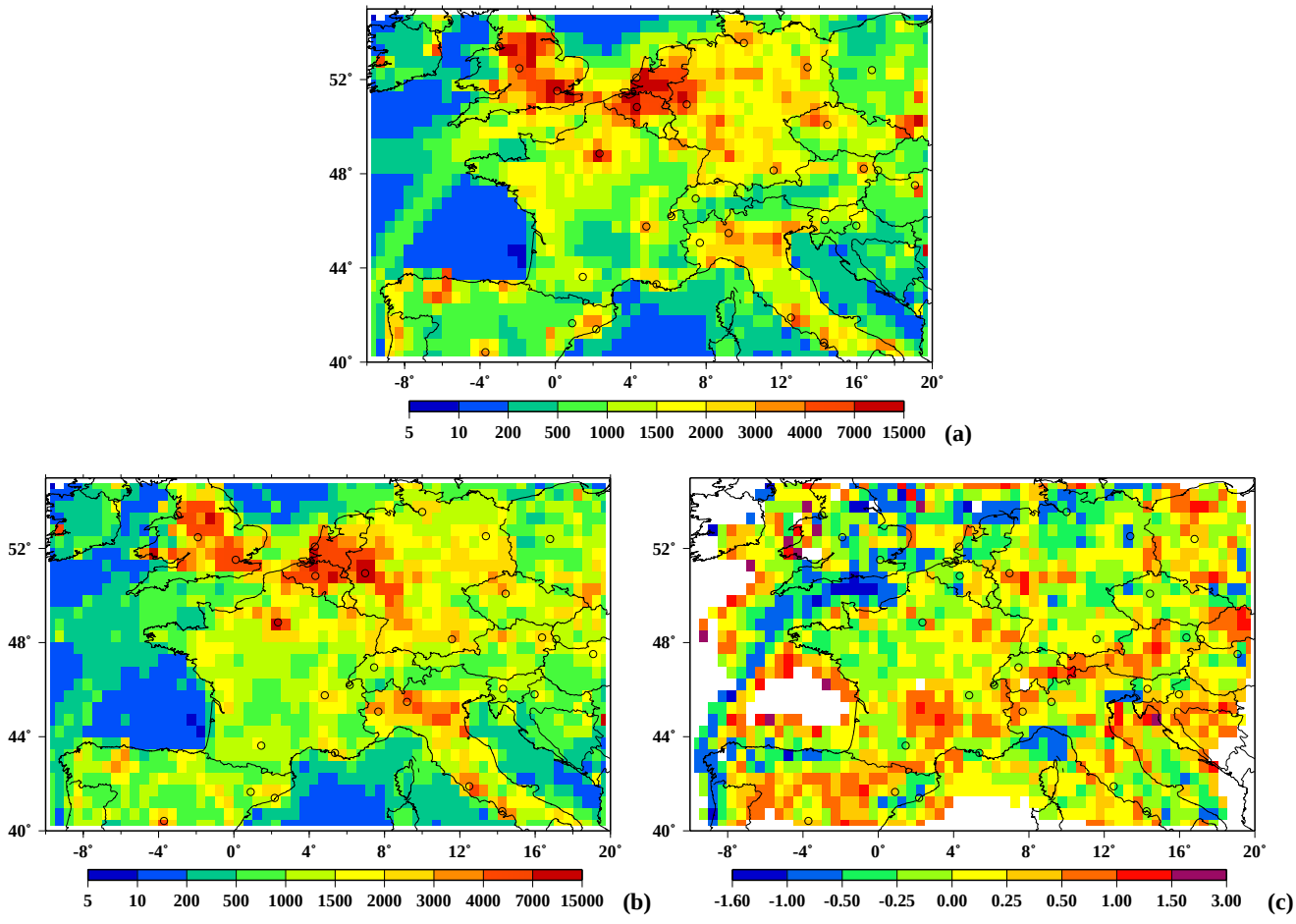

Fig. 7. The a priori **(a)** and a posteriori **(b)** estimates for total (biogenic plus anthropogenic) emissions (in molecules$\times$cm$^{-2}\times$s$^{-1}\times 10^8$) averaged over summer months (June–August) of 2001, and also the natural logarithms of the ratio of the a posteriori to the a priori emission estimates **(c)**. The a posteriori emissions have been obtained with GOME NO_2 columns deconvoluted with SCIAMACHY data.

in 2001) than the GOME data. Larger uncertainty of observations leads to smaller differences between the a posteriori and the a priori emissions. The blank areas in Figs. 7 and 8 correspond mostly to relatively unpolluted regions excluded from analysis in accordance with the criterion specified in Sect. 3.1 and also, for a minor part, to regions for which SCIAMACHY data were absent (see Fig. 2).

It is evident that despite significant quantitative differences, all the datasets give qualitatively similar results. In particular, in accordance to our results, the a priori emissions are probable to be persistently overestimated over Great Britain, a northwestern part of France, northern Germany and Netherlands but underestimated over northern Italy, southern France, western Germany and Spain. There is also a probable strong overestimation of NO_x emissions over sea areas corresponding to major ship tracks.

Although for almost a half of grid cells (48%), corrections are below 0.25 (about a factor 1.3, yellow and light green colour in Fig. 7c), a still important number of grid cells (26%) shows corrections larger than 0.5 (about a factor of 1.7, orange, red and blue colour). Note that on the whole, positive and negative corrections are balanced, because systematic differences between simulated and observed columns have been removed previously.

Table 1 presents the a priori and a posteriori emission estimates for several major European cities. Since the spatial resolution of our retrievals is insufficient for estimation of emissions exactly within official city boundaries, we present, instead, the emission estimates averaged over four grid cells closest to the city centre. Such kind of data is rather easy to use for inter-comparison with similar results of future inverse modelling studies and emission inventories. Our results show, in particular, that the a priori emission estimates for major cities are, on the average, relatively accurate. Indeed, the a priori estimates are outside of the range of uncertainty of the a posteriori emissions (in terms of the 68% confidence level) only for 8 from 29 cities considered. The statistically significant underestimations of NO_x emissions

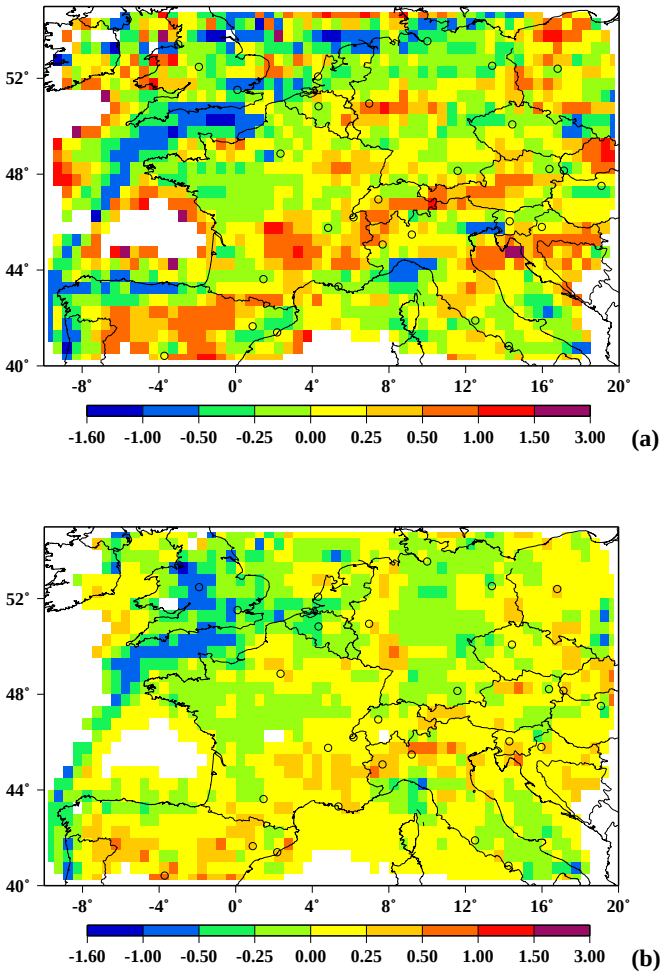

Fig. 8. Natural logarithms of the ratio of the a posteriori and a priori emissions estimates in the cases with **(a)** GOME NO_2 columns deconvoluted with simulated NO_2 columns (by CHIMERE) and **(b)** NO_2 columns derived from SCIAMACHY measurements in 2004.

Table 1. A priori and a posteriori estimates of NO_x emission rates in some European cities. The reported values represent anthropogenic emission rates (molecules$\times$cm$^{-2}\times$s$^{-1}\times 10^{11}$) averaged for three summer months (June to August) of 2001 and over four model's grid cells closest to the city center. The uncertainties in the a priori emissions are assumed to be the same for any grid of the model and are estimated to be about 1.9 (in terms of the geometric standard deviation), while the uncertainties in the a posteriori emissions are given in the brackets. For some cities (as Cologne), other big cities may contribute to the emissions.

City	A priori	A posteriori
Barcelona	2.79	1.95 (1.2)
Berlin	2.25	1.56 (1.4)
Bern	0.98	1.01 (1.3)
Birmingham	5.07	4.56 (1.2)
Bratislava	1.09	1.12 (1.3)
Brussels	5.00	4.83 (1.3)
Budapest	2.31	2.16 (1.3)
Cologne	5.64	6.18 (1.4)
Geneva	1.04	1.14 (1.3)
Hague	7.25	6.84 (1.4)
Hamburg	2.33	1.69 (1.3)
Liverpool	3.69	3.37 (1.6)
Ljubljana	1.05	1.14 (1.3)
London	7.76	4.75 (1.4)
Lyon	1.73	1.65 (1.2)
Madrid	2.23	2.73 (1.2)
Marseille	1.93	1.68 (1.2)
Milan	3.13	3.37 (1.2)
Munich	2.03	1.93 (1.2)
Naples	1.98	2.25 (1.1)
Paris	4.68	3.92 (1.3)
Poznan	0.57	0.69 (1.3)
Prague	2.18	2.09 (1.2)
Rome	3.20	3.28 (1.2)
Toulouse	0.86	0.74 (1.3)
Turin	1.41	2.29 (1.3)
Vienna	1.87	1.69 (1.3)
Zagreb	1.15	0.88 (1.3)
Zaragoza	1.41	1.36 (1.5)

are found in Madrid, Naples and Turin, while overestimations are detected in Barcelona, Berlin, Hamburg, London and Zagreb. It is interesting to note also that, on the whole, the most of the cities (about 62%) have lower a posteriori than a priori emissions.

The key aspect of the emission estimates derived using inverse modelling technique is their uncertainty. Specifically, any difference between the a posteriori and a priori emissions makes little physical sense, unless that difference is statistically significant. The random uncertainties of the a posteriori (anthropogenic) emissions obtained with the "standard" set of satellite data are depicted in Fig. 9a. The mean of uncertainties is about 0.36, 68 percent of values are less than 0.4. The magnitudes of uncertainties for a given grid cell depend, mainly, on sensitivity of the NO_2 columns in nearby grid cells to emissions changes in this cell. These sensitivities depend, in turn, on magnitudes of emissions in the larger number of surrounding grid cells. Accordingly, the final picture is rather complex, but, typically, the uncertainty is smaller for more strongly polluted regions. Figure 9b distinguishes between statistically significant and insignificant emission corrections. It shows the ratio of the difference between the logarithms of a posteriori and a priori emissions to the uncertainty (at the 68% confidence level) of the a posteriori estimates. Dark areas correspond to statistically insignificant changes. Although the uncertainties in our estimates are rather large (due to uncertainties in data and model errors), we have found that the changes in the a priori emissions are statistically significant for the majority (58%) of the grid cells. Finally, Fig. 9c shows the statistical significance of a

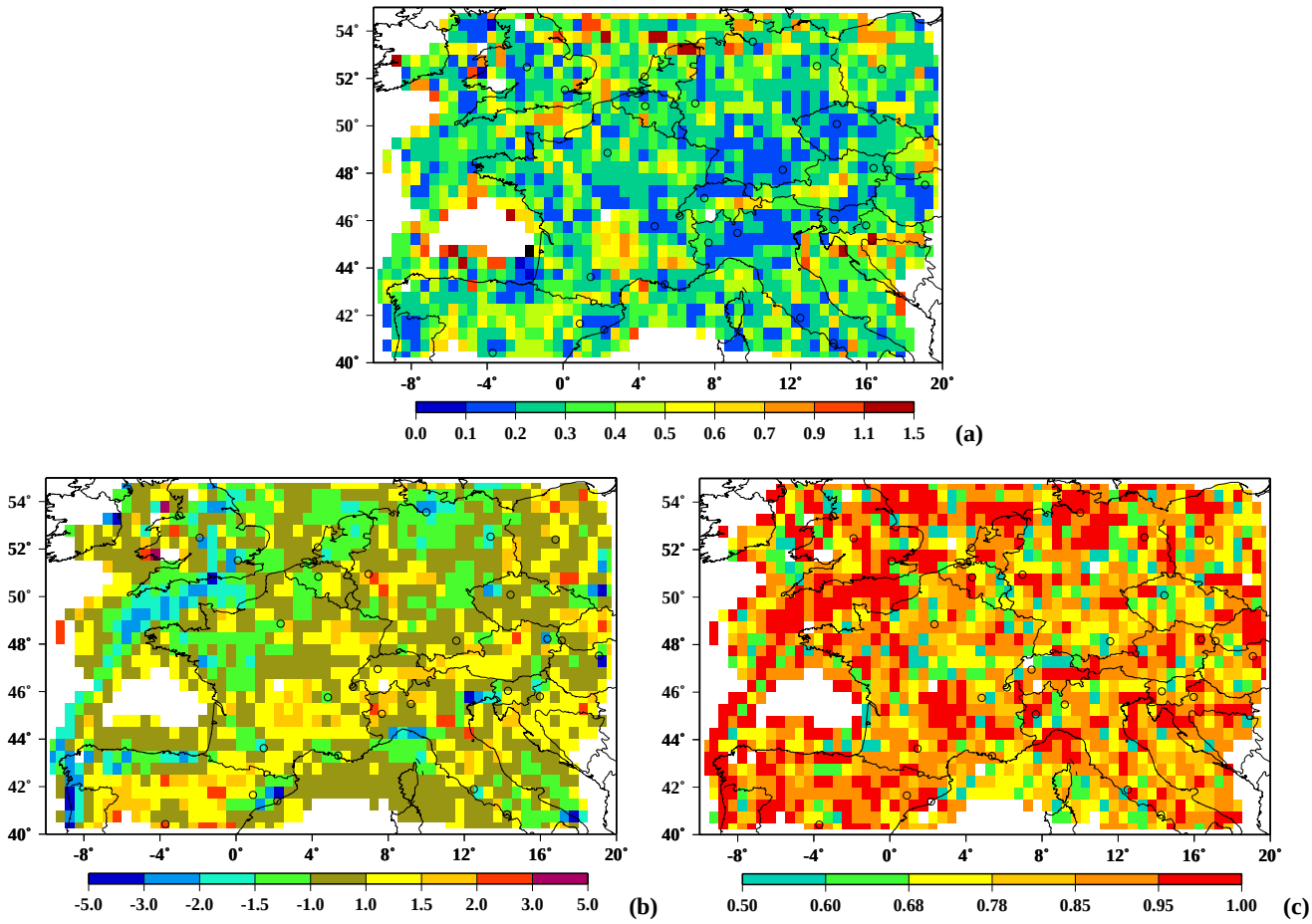

Fig. 9. (a) The uncertainties (standard deviations) in the natural logarithms of the a posteriori anthropogenic emissions; **(b)** The ratio of the difference between the natural logarithms of the a posteriori and a priori emissions to the uncertainty of the a posteriori estimates; **(c)** The statistical significance of the direction of the a priori emission corrections. All the results correspond to the case of GOME NO_2 columns deconvoluted with SCIAMACHY data.

Table 2. Estimates for the uncertainties in the anthropogenic NO_x emissions and NO_2 columns. The uncertainties in NO_x emissions and NO_2 columns are quantified in terms of the 68.3 % confidence level for the natural logarithms of the respective values. All values are dimensionless. Data sets: 1) the GOME data deconvoluted with NO_2 columns from SCIAMACHY, 2) the GOME data deconvoluted with simulated NO_2 columns, 3) the NO_2 columns derived from SCIAMACHY measurements in 2004.

data set	σ_e		σ_c
	a priori	a posteriori	
1	0.62 (±0.08)	0.36	0.18 (±0.17)
2	0.55 (±0.26)	0.35	0.15 (±0.14)
3	0.41 (±0.22)	0.28	0.29 (±0.13)

more robust estimate expressed in terms of the direction of the a priori emission corrections; that is, whether the a priori emissions should be increased of decreased. These estimates and their uncertainty have been obtained as an independent output of our Monte Carlo experiment. In this case, the total fraction of statistically significant estimates is much larger and reaches 86%. All the results presented in Figs. 7–9 are available in the digital form upon request.

Table 2 presents our estimates for uncertainties in the natural logarithms of the a priori and a posteriori anthropogenic NO_x emissions and NO_2 columns. In the Monte Carlo procedure, the standard deviations for the a priori emissions and columns have been treated as random variables, so that we could get not only estimates of their values but also the uncertainties of these estimates, which are given in the brackets. In particular, the uncertainty of the a priori emissions is estimated to be about 0.62 and the uncertainty in the a posteriori emissions in the main case is estimated to be 42% lower

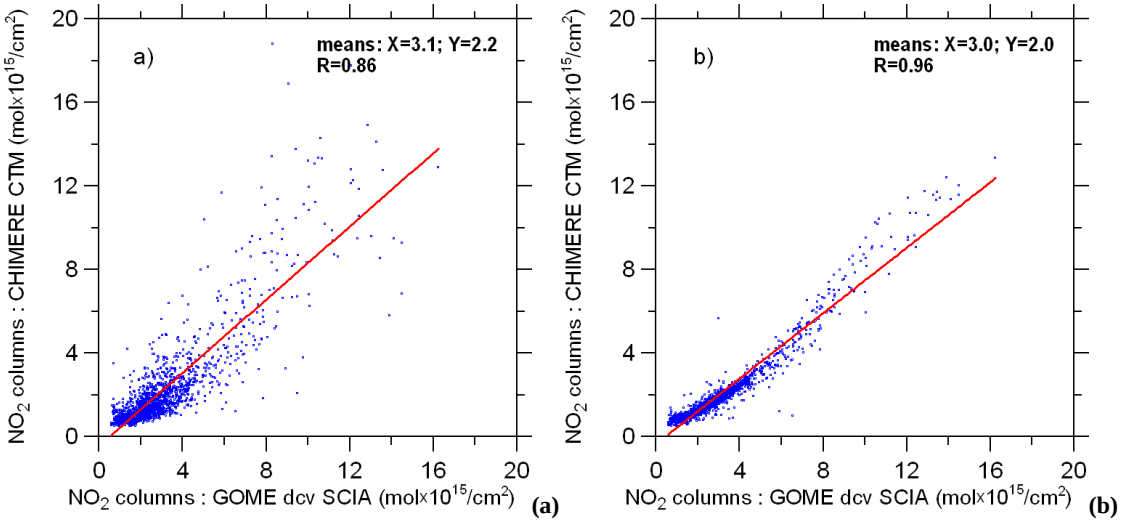

Fig. 10. The NO_2 columns derived from GOME measurements and deconvoluted with NO_2 columns from SCIAMACHY versus the modelled NO_2 columns calculated with **(a)** the a priori and **(b)** the a posteriori emissions. All data shown represent averages over three summer months of 2001.

(0.36). Expressed in terms of the geometric standard deviation, the uncertainties of the a priori and a posteriori emissions are about 1.9 and 1.4, respectively. It is useful to note that estimates of the standard deviation of the priori emission in the cases of alternative datasets for NO_2 columns, are not inconsistent with the corresponding estimate for the standard case, taking into account the large uncertainty of the estimates obtained with the alternative datasets. The estimates of the uncertainty in NO_2 columns are very uncertain, but they are always smaller than uncertainties for a priori emissions. Note that the estimates of the standard deviation of the a posteriori emissions may also be uncertain. Although our procedure does not enable evaluation of this uncertainty, it seems reasonable to believe that it is of the same order of magnitude as the uncertainty of the standard deviation of a priori emissions. If it is indeed so, actual uncertainties of the a posteriori emissions in the cases of both SCIAMACHY and GOME data deconvoluted with CHIMERE may be much larger than their estimates given in Table 2.

It should be kept in mind that all the results presented above address only a random part of the uncertainties in NO_x emissions and NO_2 columns. Systematic errors are not evaluated in this study. Nonetheless, it seems reasonable to hypothesize that they are much smaller than the random uncertainties. Indeed, the procedure of derivation of the gridded EMEP emission data involves different kinds of scaling from the national totals to the gridded estimates (see e.g., Vestreng, 2004). Errors in emissions factors for specific activities may have an important impact on emission estimates for specific grid cells (where these activities are dominant), but these errors likely tend to average out over the model domain. If the hypothesis that the random errors are dominating is correct, then the interpretation of our results is very straightforward: the systematic errors can be simply neglected. Otherwise, it is necessary to keep in mind that both the a priori and a posteriori emissions can be uniformly biased and that our uncertainty estimates do not include possible systematic errors.

4.2 Checking agreement between measured and modelled data

The correction of emissions should lead to improvement in the agreement between modelled and measured data, although only part of the discrepancy between simulated and observational data may be due to uncertainty in emissions. In order to check the improvement in the agreement between the observational and simulated data discussed above, we have re-run CHIMERE with the corresponding new emissions. The significant improvement of agreement between the measured and modelled NO_2 columns in the standard case is demonstrated in Fig. 10. In particular, the correlation coefficient has increased from 0.85 to 0.96. We have also evaluated the debiased root mean squared error,

$$\mathrm{RMSE} = \left(\frac{1}{N} \sum_{i=1}^{N} \left(c_o^i - c_m^i - \delta_c^i \right)^2 \right)^{1/2}, \qquad (21)$$

which has been reduced from 0.44 to 0.19. It is important to note that the residual uncertainty of the NO_2 columns is in perfect agreement with its estimation (σ_c) obtained using the linear statistical models (12) (see Table 2). This observation counts in favour of sufficient accuracy of our inversion procedure.

Obviously, the improvement in agreement between the simulated and measured NO_2 columns does not necessarily

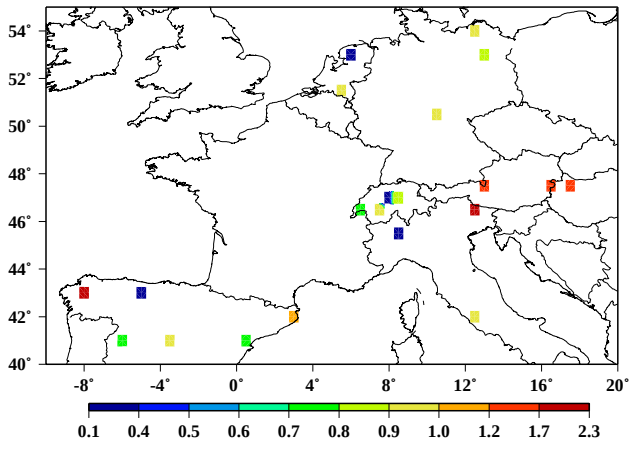

Fig. 11. The absolute values of ratios of the "a posteriori" and "a priori" biases defined as the differences between the average values of the modelled and observed NO_2 concentrations for a given EMEP site. The a posteriori emissions enable the reduction of biases at 15 stations out of 21.

mean that the a posteriori emissions are actually better than the a priori ones, because these observations have been used directly to fit the emission data. The improvement in agreement between the modelled and measured near surface concentrations provides a more critical test for our a posteriori emissions, since these data have not been used directly for fitting NO_x emissions. We found that the improved emissions enable reduction of the biases for the near surface concentrations at 15 stations out of 21. The biases are defined simply as the differences between measured and modelled concentrations. A simple statistical test shows that if the result of inversion were equivalent to adding random errors to the modeled NO_2 concentrations, then the probability that the biases are reduced at 15 stations from 21 would be less than 0.1. Hence, the obtained improvement is statistically significant with the probability of error less than 10 percent. The absolute values of ratios of the "a posteriori" and a priori biases are shown in Fig. 11.

The RMSE defined in terms of concentration logarithms similar to Eq. (21) has reduced from 0.63 to 0.56. The same numbers have been obtained using the linear approximation (12, 13). Evidently, the reduction of RMSE in the case of NO_2 surface concentrations is much smaller than that in the case of NO_2 columns, but this may be mainly due to the fact that uncertainties in NO_2 near surface concentrations (either measured or simulated) that are not caused by uncertainties in emissions are significantly larger than uncertainties in NO_2 columns. Indeed, if errors in the logarithms of NO_2 concentrations (related or not to uncertainties in emissions) are normally distributed and independent, then squares of errors are additive. Using our model we have found that if the uncertainty of NO_x emissions were about 0.6 and if other sources of errors of NO_2 concentrations were absent, the corresponding RMSE for near surface NO_2 concentrations would be about 0.3 (instead of 0.63). Then RMSE due to not emission related errors would be 0.55 ($[0.63^2–0.3^2]^{0.5}$). Thus the observed reduction of RMSE from 0.63 to 0.56 implies that errors caused by uncertainties in the a posteriori emissions should be very small. The RMSE corresponding to only this part of uncertainties would be less than 0.1 (instead of 0.3). This corresponds indeed to a strong reduction in the part of error related to emissions. Therefore, we can conclude that our inverse modelling procedure has actually corrected the major part of the discrepancy between the observed and modelled NO_2 concentrations caused by uncertainties of emissions.

4.3 Discussion

Since the inverse modeling of emissions is based on the use of a chemistry transport model and involves some assumptions about statistical properties of the errors in the model and in input data, the inverse modeling results are accurate only as much as the model is correct and the underlying assumptions are valid. In this sense, the inverse modeling is rather similar to more traditional "forward" modeling, especially in those applications of the latter where the results cannot be easily validated by comparison with available observations (for example, in sensitivity and prognostic studies). Accordingly, any inverse modeling scheme may be regarded as a special kind of a model that evaluates some physical characteristics (usually those unobserved directly) given values of other (measured) characteristics. When simulated results cannot be easily verified using observations, one can use other ways of estimating their uncertainties. One way involves Monte-Carlo experiments and is employed in our study. Alternatively, the uncertainties could be estimated using the methods of ensemble modeling, which are nowadays frequently used in climatological studies (e.g., National Assessment Synthesis Team, 2001). In any case, since indirect ways of estimating uncertainties of the simulated results are based on current understanding of a considered system, possible sources of uncertainties and their properties, the estimated uncertainties may be still different from the true ones.

In this study, we have attempted to get more information on the uncertainties of input data directly from observations. However, in doing so we have still involved the model and made some important assumptions about statistical properties of errors, which seem to be reasonable but are difficult to verify. In particular, we have assumed that errors of NO_2 columns and near-surface concentrations are statistically independent. While the measurement errors are certainly independent, the statistical independence of model errors is less obvious. The positive or negative covariance between the errors of modelled columns and concentration would lead to under- or overestimation of σ_c and over- or underestimation of σ_e, respectively. Errors caused by inaccuracies in representation of chemical processes and horizontal transport may

be common for both columns and concentrations. However, errors in vertical mixing are likely to anti-covariate, because, for example, the overestimation of the mixing would lead to larger columns (as discussed, e.g., by Savage et al., 2005) but lower concentrations. It is also likely that a major part of the discrepancy between the modeled and measured in situ NO_2 concentrations is caused by insufficient spatial resolution of CHIMERE. Otherwise, it is difficult to explain why RMSE in the case of the ground based data is much higher than that in the case of satellite data (see the previous section), whereas the satellite data are expected to be less certain than the data of ground based measurements.

Another important assumption underlying our inverse modelling scheme is that random errors of both columns and concentrations are independent between different grid cells. In the lack of any prior information about spatial covariations of the errors, such an assumption seems to be really the best option. Nevertheless, our results are conditional on this assumption. Such kind of conditioning of results of Bayesian inference on a priori assumptions is usual and, in fact, inevitable. Inverse modelling (as well as any kind of the modelling) is intended to improve the current (a priori) knowledge by enriching it with observational information, rather than to provide the "absolute truth". Although our results show (see Fig. 7c) that the errors of a priori emissions are probable to covariate in some way, these covariations is the new (a posteriori) knowledge that could not be used for elaborating the a priori assumptions.

An interesting point is why the errors of emissions may be distributed in such semi-regular way. One plausible explanation is that if different regions feature different kinds of predominant industrial or agricultural activity, the emission error covariations may reflect some common uncertainties for specific types of activity. For example, in accordance to EMEP data (Vestreng et al., 2004) the emissions attributed to the 1st SNAP sector (combustion in energy and transformation industries) constitute 25% of total anthropogenic NO_x emissions in the United Kingdom, but only 11% in Italy. Another example is NO_x emissions from ships in the northwest of Europe, which, in accordance to our results, are likely to be strongly overestimated in EMEP data. However, this explanation of spatial covariations of errors in the a priori emissions is only a hypothesis, which needs to be verified in future studies. It is also not inconceivable that the covariations of errors in a priori emissions are, in some cases, artefacts of spatial covariations of errors in modelled or measured NO_2 columns. Even if the uncertainties for a posteriori emissions are, on the average, considerably smaller than those for a priori emissions, this may not be true for specific grid cells or regions with covariating corrections.

The results presented above lead us to believe that the a posteriori emission estimates are considerably more certain than the a priori emissions prescribed in the model. Although these new estimates cannot be regarded as a better substitute for the data of the EMEP emission inventory (as our results concern emission averages for three summer months rather than their yearly averages), they can be used as an alternative emission data set for CHIMERE and other CTMs for Western Europe. Indeed, regional CTMs are mainly designed to simulate the photooxidant pollution, which is strongest during the warm season. Similarly, although we have not estimated the uncertainty in the yearly EMEP emissions, our estimation of the uncertainty in the summer emissions used in CHIMERE and other CTM's is a useful result in itself, which can, for example, be used in sensitivity studies.

5 Conclusions

We have studied the benefits of using tropospheric NO_2 column amounts derived from GOME and SCIAMACHY measurements for improving available estimates of NO_x emissions used in a continental scale CTM. We set-up an original inverse modelling scheme that (1) is based on Bayesian approach, (2) combines the data of satellite measurements of tropospheric NO_2 columns with data of ground based measurements of near-surface NO_2 concentration, (3) involves a simple approximation of the modelled relationships between NO_2 columns/concentrations and NO_x emissions, which drastically reduces the computational demand of the problem, and (4) includes a special Monte Carlo experiment. Using this scheme, we have derived an improved spatial distribution of NO_x emissions for Western Europe and for the summer season. We have also estimated the magnitudes of uncertainties in input and output data, using information contained in measurement data. Specifically, we have found that the the random part (in the spatial sense) of uncertainty in the anthropogenic NO_x emissions that were derived from EMEP annual data and that are currently used in the CHIMERE CTM is about 0.6 (in terms of the standard deviation of the emission rate natural logarithms). The uncertainty in our a posteriori emissions is estimated to be about 40% lower. As it is unavoidable in inverse modelling studies, the obtained degree of uncertainty reduction is conditional of some assumptions used in the inversion algorithm. They mainly concern the independence of different types of errors (emissions, model, surface, columns and surface measurements) and the independence for different grid cells. The distinctive feature of our study is that we do not make any quantitative assumptions regarding the magnitudes of uncertainties in input data and in a priory emission that are common in other studies.

The improved emissions enable strong reduction of the discrepancy between measured and modelled NO_2 columns (more than two times in terms of RMSE). The reduction of the differences between measured and modelled NO_2 near-surface concentrations is less considerable (about 10%), but it is argued that this improvement is necessarily smaller because of the predominance of other errors sources than emissions.

We also have found that corrections in a priori emissions are distributed rather irregularly on a large scale but tend to covariate on smaller regional scales. In particular, in accordance to our results, the a priori emissions are probable to be persistently overestimated over Great Britain, North-West of France, northern Germany and Netherlands but underestimated over northern Italy, southern France and Spain. For these regions, corrections are typically about several tenths of percent. It still remains unknown whether these probable inaccuracies in a priori emissions are due to uncertainties in EMEP annual emission averages or due to inaccuracy in their temporal profile assigned in the model. It is also an open question whether uncertainties in a priori emissions can be attributed to definite source categories. Accordingly, our results concerning differences between a posteriori and a priori emissions only give guesses about possible inaccuracies in emission inventories data, rather than indicating real flaws. Nevertheless, our a posteriori emission estimates can be used directly for assigning emission parameters in CHIMERE and other similar CTMs for Western Europe.

Our study also showed that in spite of uncertainties in available satellite data for tropospheric NO_2 columns, they are useful for improving our current knowledge on NO_x sources even on the relatively fine spatial scales resolved by a typical continental scale CTM. The principal methodological difficulty that seriously hampers further progress in inverse modelling studies and practical utilization of their results relates to insufficient information on the character and magnitudes of uncertainties in available emissions estimates, satellite data, and model results. We have suggested that useful information about all these uncertainties can be obtained by combining different sources of measurement data. Note that only random errors (in a spatial sense) could be further characterised, but not systematic errors. Thus, an unavoidable limitation of our study is not to be able to correct systematic (again in a spatial sense) errors in emissions. However, we have argued that systematic errors should be much smaller than random errors which can be corrected.

In this study, we only have made the first step in the promising direction of inverse modelling of NO_x emissions on a regional scale using satellite measurements. Future steps could include the involvement of other sources of observational information, such as the data of ozone monitoring or aircraft measurements of related pollutants. In addition, future studies could put a stronger focus on the temporal evolution of emissions on various time scales (type of the day, seasonal, interannual).

Acknowledgements. I. B. Konovalov acknowledges the support of Centre National de la Recherche Scientifique (CNRS) and NATO Science Fellowships Sub-Programme. The support for this study was also provided by Russian Foundation for Basic Research, grant No. 05-05-64365-a and by Russian Academy of Sciences in the framework of the Programme for Basic Research "Physics of Atmosphere; Electrical Processes, Radiophysical Methods of Research". GOME raw data were provided by ESA through DFD/DLR. Analysis of the GOME data was supported by the European union under contract EVk2-CF1999-00011 (POET) and the University of Bremen.

Edited by: M. Dameris

References

Aas, W., Hjellbrekke, A.-G., and Schaug, J.: Data quality 1998, quality assurance, and field comparisons, EMEP/CCC-Report 6/2000, NILU, 2000.

Aumont, B., Jaecker-Voirol, A., Martin, B., and Toupance, G.: Tests of some reduction hypotheses made in photochemical mechanisms, Atmos. Environ., 30, 2061–2077, 1997.

Beekmann, M. and Derognat, C.: Monte Carlo uncertainty analysis of a regional-scale transport chemistry model constrained by measurements from the Atmospheric Pollution Over the Paris Area (ESQUIF) campaign, J. Geophys. Res., 108(D17), 8559, doi:10.1029/2003JD003391, 2003.

Bessagnet, B., Hodzig, A., Vautard, R., Beekmann, M., Cheinet, S., Honore, C., Liousse, C., and Rouil, L.: Aerosol modeling with CHIMERE – preliminary evaluation at the continental scale, Atmos. Environ., 38, 2803–2817, 2004.

Boersma, K. F., Eskes, H. J., and Brinksma, E. J.: Error Analysis for Tropospheric NO_2 Retrieval from Space, J. Geophys. Res., 109, D04311, doi:10.1029/2003JD003962, 2004.

Boersma, K. F. Eskes, H. J., Meijer, E. W., Kelder, H. M.: Estimates of lightning NO_x production from GOME satellite observations, Atmos. Chem. Phys., 5, 2311–2331, 2005.

Bovensmann, H., Burrows, J. P., Buchwitz, M., Frerick, J., Noel, S., Rozanov, V.-V., Chance, K. V., and Goede, A. P. H.: SCIAMACHY: Mission Objectives and Measurement Modes, J. Atmos. Sci., 56, 127–150, 1999.

Bradshaw, J., Davis, D., Grodzinsky, G., Smyth, S., Newell, R., Sandholm, S., and Liu, S.: Observed distributions of nitrogen oxides in the remote free troposphere from NASA Global Tropospheric Experiment programs, Rev. Geophys., 38, 61–116, 2000.

Buchwitz, M., Noël, S., Bramstedt, S., Rozanov, V. V., Bovensmann, H., Tsvetkova, S., and Burrows, J. P.: Retrieval of trace gas vertical columns from SCIAMACHY/ENVISAT near-infrared nadir spectra: First preliminary results, Adv. Space Res., 34, 809–814, 2004.

Burrows, J. P., Weber, M., Buchwitz, M., Rozanov, V., Ladstätter-Weißenmayer, A., Richter, A., DeBeek, R., Hoogen, R., Bramstedt, K., Eichmann, K.-U., Eisinger, M., and Perner, D.: The Global Ozone Monitoring Experiment (GOME): Mission concept and first scientific results, J. Atmos. Sci., 56, 151–175, 1999.

Carter, W. P. L.: A detailed mechanism for the gas-phase atmospheric reactions of organic compounds, Atmos. Environ., 24, 481–518, 1990.

Chipperfield, M. P.: Multiannual simulations with a three-dimensional chemical transport model, J. Geophys. Res., 104, 1781–1805, 1999.

Derognat, C.: Pollution photo-oxydante à l'échelle urbaine et interaction avec l'échelle régionale, thèse de doctorat, Université Pierre et Marie Curie, Paris 6, France, Avril 2002.

EMEP-CORINAIR Emission Inventory Guidebook, EEA Technical report No 30, European Environment Agency, 2005.

Enting, I. G.: Inverse Problems in Atmospheric Constituents transport, Cambridge University Press, 2002.

Eisinger, M. and Burrows, J. P.: Tropospheric Sulfur Dioxide observed by the ERS-2 GOME instrument, Geophys. Res. Lett., 25, 4177–4180, 1998.

Gardner, M. W. and Dorling, S. R.: Artificial neural networks (the multilayer perceptron) – A review of applications in the atmospheric sciences, Atmos. Environ., 32, 2627–2636, 1998.

GENEMIS (Generation of European Emission Data for Episodes) project: EUROTRAC Annual Report 1993, Part 5, EUROTRAC International Scientific Secretariat, Garmisch-Partenkirchen, Germany, 1994.

Giering, R.: Tangent linear and adjoint biogeochemical models, in: Inverse methods in Global Biogeochemical Cycles, edited by: Kasibhatla, P. S., Geophysical Monograph, American Geophysical Union, 114, p. 33–48, 2000.

Heimann, M. and Kaminski, T.: Inverse modeling approaches to infer surface trace gas fluxes from observed atmospheric mixing ratios, in: Approaches to scaling of trace gas fluxes in ecosystems, edited by: Bouwman, A. F., Elsevier, Amsterdam, ch. 14, p. 275–295, 1999.

Heue K.-P., Richter A., Bruns M., Burrows J. P., Friedeburg C. V., Platt U., Pundt I., Wang P., Wagner T. : Validation of SCIAMACHY tropospheric NO_2-columns with AMAXDOAS measurements, Atmos. Chem. Phys., 5, 1039–1051, 2005.

Hornik, K., Stinchcombe, M., and White, H.: Multilayer feedforward networks are universal approximators, Neural Networks, 2, 359–366, 1989.

Horowitz, L. W., Walters, S., Mauzerall, D. L., Emmons, L. K., Rasch, P. J., Granier, C., Tie, X., Lamarque, J.-F., Schultz, M. G., Tyndall, G. S., Orlando, J. J., and Brasseur, G. P.: A global simulation of ozone and related tracers: description and evaluation of MOZART, Version 2, J. Geophys. Res., 108(D24), 4784, doi:10.1029/2002JD002853, 2003.

Houweling, S., Kaminski, T., Dentener, F., Lelieveld, J., and Heimann, M.: Inverse modelling of methane sources and sinks using the adjoint of a global transport model, J. Geophys. Res., 104, 26 137–26 160, 1999.

Kaminski, T., Heimann, M., and Giering, R.: A coarse grid three-dimensional global inverse model of the atmospheric transport, 2, Inversion of the transport of CO in the 1980s, J. Geophys. Res., 104, 18 555–18 581, 1999.

Kley, D., Kleinmann, M., Sanderman, H., and Krupa, S.: Photochemical oxidants: state of science, Environ. Pollut., 100, 19–42, 1999.

Koelemeijer, R. B. A., Stammes, P., Hovenier, J. W., and de Haan, J. F.: A fast method for retrieval of cloud parameters using oxygen A band measurements from the Global Ozone Monitoring Experiment, J. Geophys. Res., 106, 3475–3490, 2001.

Koelemeijer, R. B. A., de Haan, J. F., and Stammes, P.: A database of spectral surface reflectivity in the range 335–772 nm derived from 5.5 years of GOME observations, J. Geophys. Res., 108(D2), 4070, doi:10.1029/2002JD002429, 2003.

Konovalov, I. B.: Application of neural networks for studying nonlinear relationships between ozone and its precursors, J. Geophys. Res., 107(D11), doi:10.1029/2001JD000863, 2002.

Konovalov, I. B., Beekmann, M., Vautard, R., Burrows, J. P., Richter, A., Nüß, H., and Elansky, N.: Comparison and evaluation of modelled and GOME measurement derived tropospheric NO_2 columns over Western and Eastern Europe, Atmos. Chem. Phys., 5, 169–190, 2005.

Kühlwein, J. and Friedrich, R.: Uncertainties of modelling emissions from road transport, Atmos. Environ., 34, 4603–4610, 2000.

Kühlwein, J., Friedrich, R., Kalthoff, N., Corsmeier, U., Slemr, F., Habram, M., and Möllmann-Coers, M.: Comparison of modelled and measured total CO and NO_x emission rates, Atmos. Environ., 36, suppl. 1, S53–S60, 2002.

Labrador, L. J., von Kuhlmann, R., and Lawrence, M. G.: The effect of lightning-produced NO_x and its vertical distribution on atmospheric chemistry: sensitivity simulations with MATCH-MPIC, Atmos. Chem. Phys., 5, 1815–1834, 2005.

Latuatti, M.: Contribution à l'étude du bilan de l'ozone troposphérique à l'interface de l'Europe et de l'Atlantique Nord: Modélisation lagrangienne et mesures en altitide, PhD thesis, Universit/'e Paris 6, Paris, 1997.

Lee, D. S., Köhler, I., Grobler, E., Rohrer, F., Sausen, R., Gallardo-Klenner, L., Olivier, J. J. G., and Dentener, F. D.: Estimations of global NOx emissions and their uncertainties, Atmos. Environ., 31, 1735–1749, 1997.

Levelt, P. F., van den Oord, B., Hilsenrath, E., Leppelmeier, G. W., Bhartia, P. K., Malkki, A., Kelder, H., van der A, R. J., Brinksma, E. J., van Oss, R., Veefkind, P., van Weele, M., and Noordhoek, R.: Science Objectives of EOS-Aura's Ozone Monitoring Instrument (OMI), Proc. Quad. Ozone Symposium, Sapporo, Japan, p. 127–128, 2000.

Leue, C., Wenig, M., Wagner, T., Klimm, O., Platt, U., and Jahne, B.: Quantitative analysis of NOx emissions from GOME satellite image sequences, J. Geophys. Res., 106, 5493–5505, 2001.

Madronich, S. and Flocke, S.: The role of solar radiation in atmospheric chemistry: in: Handbook of Environmental Chemistry, edited by: Boul, P., Springer, Heidelberg, pp. 1–27, 1998.

Martin, R. V., Chance, K., Jacob, D. J., Kurosu, T. P., Spurr, R. J. D., Bucsela, E., Gleason, J. F., Palmer, P. I., Bey, I., Fiore, A. M., Li, Q. B., Yantosca, R. M., and Koelemeijer, R. B. A.: An improved retrieval of tropospheric nitrogen dioxide from GOME, J. Geophys. Res., 107(D20), 4437, doi:10.1029/2001JD001027, 2002.

Martin, R. V., Jacob, D. J., Chance, K., Kurosu, T., Palmer, P. I., and Evans, M. J.: Global inventory of nitrogen oxide emissions constrained by space-based observations of NO_2 columns, J. Geophys. Res., 108(D17), 4537, doi:10.1029/2003JD003453, 2003.

Metropolis, N., Rosenbluth, A. W., Rosenbluth, M. N., Teller, A. H., Teller, E.: Equation of State Calculations by Fast Computing Machines, J. Chem. Phys., 1, 6, 1087–1092, 1953.

Mosegaard, K. and Tarantola, A.: Probabilistic Approach to Inverse Problems, in the International Handbook of Earthquake & Engineering Seismology (Part A), Academic Press, p. 237–265, 2002.

Müller, J.-F. and Stavrakou, T.: Inversion of CO and NO_x emissions using the adjoint of the IMAGES model, Atmos. Chem. Phys., 5, 1157–1186, 2005.

National Assessment Synthesis Team: Climate Change Impacts on the United States: The Potential Impacts of Climate Variability and Change. Cambridge University Press, 618 pp., 2001.

Passant, N. R.: Speciation of UK emissions of non-volatile organic, AEA Technology, NETCEN, AEAT/ENV/R/0545, Culham, 2002.

Petron, G., Granier, C., Khattatov, B., Lamarque, J. F., Yudin, V., Müller, J. F., and Gille, J.: Inverse modeling of carbon monoxide surface emissions using climate monitoring and diagnostics laboratory network observations, J. Geophys. Res., 107(D24), 4761, doi:10.1029/2001JD001305, 2002.

Press, W. H., Teukolsky, S. A., Vetterling, W. T., and Flannery, B. P.: Numerical Recipes, 2nd edition, Cambridge University Press, 1992.

Richter, A.: Absorptionsspektroskopische Messungen stratosphärischer Spurengase über Bremen, 53° N, PhD thesis (in German), University of Bremen, June, 1997.

Richter, A. and Burrows, J. P.: Tropospheric NO_2 from GOME measurements, Adv. Space Res., 29, 1673–1683, 2002.

Richter, A., Burrows, J. P., Fietkau, S., Medeke, T., Notholt, J., Oetjen, H., Sierk, B., Warneke, T., Wittrock, F., Dix, B., Friess, U., Wagner, T., Blumenstock, T., Griesfeller, A., Sussmann, R., Rockmann, A., and Schulz, A.: A scientific NO_2 product from SCIAMACHY: First results and validation, Proceedings of the ESA ACVE 2 workshop in Esrin, Italy, 2004.

Richter, A., Burrows, J. P., Nüß, H., Granier, C., and Niemeier, U.: Increase in Tropospheric Nitrogen Dioxide Over China Observed from Space, Nature, 437, 129–132, doi:10.1038/nature04092, 2005.

Savage, N., Law, K., Pyle, J., Richter, A., Nüß, H., and Burrows, J.: Using GOME NO_2 satellite data to examine regional differences in TOMCAT model performance, Atmos. Chem. Phys., 4, 1895–1912, 2004.

Schmidt, H. C., Derognat, C., Vautard, R., and Beekmann, M.: A comparison of simulated and observed ozone mixing ratios for the summer of 1998 in western Europe, Atmos. Environ., 35, 6277–6297, 2001.

Simpson, D., Winiwarter, W., Borjesson, G., Cinderby, S., Ferreiro, A., Guenther, A., Hewitt, C. N., Janson, R., Khalil, M. A. K., Owen, S., Pierce, T. E., Puxbaum, H., Shearer, M., Steinbrecher, S., Svennson, B. H., Tarrason, L., and Oquist, M. G.: Inventorying emissions from nature in Europe, J. Geophys. Res., 104, 8113–8152, 1999.

Stohl, A., Williams, E., Wotawa, G., and Kromp-Kolb, H.: A European inventory of soil nitric oxide emissions on the photochemical formation of ozone in Europe, Atmos. Environ., 30, 3741–3755, 1996.

Solomon, S., Portmann, R. W., Sanders, R. W., Daniel, J. S., Madsen, W., Bartram, B., and Dutton, E. G.: On the role of nitrogen dioxide in the absorption of solar radiation, J. Geophys. Res., 104, 12 047–12 058, 1999.

Tarantola, A.: Inverse problem theory; methods for data fitting and model parameter estimation, Elsevier, 1987.

Tarassòn L., Jonson, J.E., Berntsen, T. K., Rypdal, K.: Study on air quality impacts of non-LTO emissions from aviation, Final report to the European Commission under contract B4-3040/2002/343093/MAR/C1, CICERO, Oslo, http://europa.eu.int/comm/environment/air/pdf/air_quality_impacts_finalreport.pdf, 2004.

Thomas, W., Hegels, E., Slijkhuis, S., Spurr, R., and Chance, K.: Detection of biomass burning combustion products in Southeast Asia from backscatter data taken by the GOME spectrometer, Geophys. Res. Lett., 25, 1317–1320, 1998.

Toenges-Schuller, N.: Globale Verteilungsmuster anthropogener Stickoxidemissionen: Vergleich und Integration von troposphaerischen Satellitenbeobachtungen und Modellrechnungen (in German), PhD thesis, Berichte des Forschungszentrums Juelich 4160, ISSN 0944-2952, 2005.

Vautard, R., Beekmann, M., Roux, J., and Gombert, D.: Validation of a hybrid forecasting system for the ozone concentrations over the Paris area, Atmos. Environ., 35, 2449–2461, 2001.

Vautard, R., Martin, D., Beekmann, M., Drobinski, P., Friedrich, R., Jaubertie, A., Kley, D., Lattuati, M., Moral, P., Neininger, B., and Theloke, J.: Paris emission inventory diagnostics from the ESQUIF airborne measurements and a chemistry transport model, J. Geophys. Res., 108(D17), doi:10.1029/2002JD002797, 2003.

Velders, G. J. M., Granier, C., Portmann, R. W., Pfeilsticker, K., Wenig, M., Wagner, T., Platt, U., Richter, A., and Burrows, J. P.: Global tropospheric NO_2 column distributions: Comparing 3-D model calculations with GOME measurements, J. Geophys. Res., 106, 12 643–12 660, 2001.

Vestreng, V., Adams, M., and Goodwin, J.: Inventory Review 2004. Emission data reported to CLRTAP and the NEC Directive, EMEP/EEA Joint Review report, EMEP/MSC-W Note 1, July, 2004.

Wagner, T. and Platt, U.: Satellite mapping of enhanced BrO concentrations in the troposphere, Nature, 395, 486–490, 1998.